Phys. Solariterr., Potsdam, No. 22 (1983) 5 - 38

METHODS TO DETERMINE THE THREE-DIMENSIONAL STRUCTURE OF SOLAR ATMOSPHERIC MAGNETIC FIELDS

(A review)

N. SEEHAFER and J. STAUDE

Central Institute of Solar-Terrestrial Physics, Solar Observatory Einsteinturm
DDR-1500 Potsdam, G. D.R., Telegrafenberg

5

39

Contents

46

52

94

1. Introduction

Magnetic fields play a key role in solar physics and in solar activity in particular. The great variety of phenomena, events, and structures observed in the solar atmosphere is mainly due to the interaction between the magnetic field and the turbulent solar plasma with its motions such as convection and differential rotation. In order to understand the physical mechanisms of any of the phenomena it is necessary to know the underlying magnetic field structure. The magnetic field even represents the interdependence between the different phenomena of solar physics providing for the necessary unification.

In situ measurements of solar magnetic fields by means of magnetometers are possible, but only in the extension of the solar corona, that is to say in the interplanetary medium: When the solar wind is blown out from the Sun, the coronal magnetic field is carried out into the space to form the interplanetary field with the shape of an Archimedian spiral. This field may be directly measured by satellites at the orbit of the Earth, but measurements have already been carried out inside the orbit of Mercury by Helios as well as beyond the orbits of Jupiter and Saturn by Pioneer and Voyager spacecraft.

Electromagnetic waves at different wavelengths carry information on magnetic field structures from the layers of their emission and transport, thus providing for the possibility of indirect measurements. Such methods require the knowledge of the basic mechanisms of wave emission and transfer and their dependence on the magnetic field, that is to say the reliability of such methods depends more or less on the assumed models and theories. In Section 2. important methods of indirect magnetic field measurements will be shortly reviewed. We shall see that the information from such observations remains incomplete, and methods of theoretical interpolation and extrapolation of such data are needed in order to get a more complete picture of the solar magnetic field structure and dynamics. A review of such methods will be the main purpose of the following sections. By no means we intend to survey all published extrapolation procedures or special magnetic field models, rather we shall outline some of the frequently used extrapolation methods in order to enable a comparison with those methods which are being developed and applied to observations in our institute.

2. Methods to measure solar magnetic fields

Various methods for studying solar magnetic fields have been reviewed in the last decade, e. g. in papers by BECKERS (1971), STAUDE (1974), and recently by STENFLO (1978). Here we shall only summarize some of the most important methods with regard to their capability of providing reliable information on the magnetic field structure at different levels of the solar atmosphere. Such information is required as boundary conditions and constraints to the theoretical models and the interpolation and extrapolation methods described in the subsequent sections.

2.1. ZEEMAN effect

Optical polarization measurements in spectral lines are the most direct way to measure solar magnetic fields. The ZEEMAN effect causes magnetoactive lines to split into several differently polarized components, the distances of which are proportional to $g \lambda^2 B$ (g is the LANDÉ factor, λ the wavelength, and B the magnetic field strength), the relative intensities and states of polarization depending on the direction of the magnetic field vector $\underset{\sim}{B}$, that is to say on the angle γ between the line of sight and $\underset{\sim}{B}$ and on the azimuth angle φ of $\underset{\sim}{B}$.

If the ZEEMAN splitting $\Delta\lambda_B$ is not too small as compared with the line width, it may be directly measured by visual or photographic methods as it has been done already by HALE (1908), but unfortunately this is only possible for photospheric concentrations of relatively strong fields such as in sunspots. Because the line width is mainly determined by the DOPPLER width $\Delta\lambda_D$ of the line absorption coefficient and $\Delta\lambda_D \sim \lambda$, we have $\Delta\lambda_B / \Delta\lambda_D \sim \lambda$, and splittings are more prominent in the infrared than at shorter wavelengths. Due to technical difficulties such measurements in the infrared have been carried out only recently (HARVEY, 1977).

More complete information is obtained by spectropolarimetry of the line contour as it is done in photoelectric magnetographs. Usually a theory of line formation in a magnetic field is required in order to derive the magnetic field parameters from the measured STOKES parameters describing the state of polarization in the line. Reviews of these theoretical means have been given by STENFLO (1971) and LAMB (1972). The theory is well elaborated for FRAUNHOFER lines formed at photospheric level so that LTE (local thermodynamic equilibrium) may be assumed, see e. g. the review by WITTMANN (1974). Even in the simplest case the measurement of all 4 STOKES parameters is connected with numerous instrumental difficulties such as the disturbing influence of instrumental polarization and scattered light, moreover, models of the atmospheric structure in the line-forming

regions must be known (BACHMANN et al., 1975). The circular polarization V is in a first approximation proportional to $B_{\parallel} = B \cos\gamma$ for weak B; it can be measured with relatively high accuracy and to some extent independently of the difficulties mentioned above, allowing for a sensitivity of the order of 1 G even at the highest spatial resolution power of some arc seconds. Therefore measurements of the longitudinal magnetic field component $B_{\parallel}$ at photospheric level provide the most reliable data till now available. Due to unresolved magnetic field fine structures it is generally not possible even in this simplest case to measure exactly the magnetic flux or the spatial average of $B_{\parallel}$, but simultaneous measurement in several selected lines yield information on the real magnetic field strength and structure.

Measurements of the two parameters of linear polarization are additionally necessary to derive the full magnetic vector, but this is much more difficult: The transverse magnetic field components enter the analysis as a second order effect resulting in a sensitivity two orders of magnitude smaller for weak transverse fields as compared with $B_{\parallel}$, moreover, the disturbing influences of Earth atmosphere, instrumentation, and uncertainties in the models now cause much more trouble. Good data on the full vector $\underset{\sim}{B}$ are therefore scarce, but in principle methods are known how to overcome at least some of these difficulties (BACHMANN et al., 1975), and improved techniques will surely help to obtain more reliable data on $\underset{\sim}{B}$ in the future.

Magnetic field studies at higher levels of the solar atmosphere (chromosphere and corona) are still more complicated. In the visible spectral range also the strong FRAUNHOFER lines such as the BALMER lines are not only formed in the chromosphere, but contain a large amount of photospheric light especially in the wings, where usually magnetic field measurements are carried out (SCHOOLMAN, 1972; ZELENKA, 1975, see also Subsection 2.3.). The difficulties are furthermore increased by numerous blends with photospheric lines in the wings of such strong chromospheric lines. Moreover, the theory of line formation is now much more complicated because non-LTE effects and strong inhomogeneities of the medium must be taken into account. Some problems of theoretical magnetograph calibration under such difficult conditions have been discussed in a separate review paper (STAUDE, 1980). More accurate data may probably be obtained by means of pure chromospheric emission lines observed in the ultraviolet from spacecraft. Such polarimetric measurements from space were first obtained during the Solar Maximum Mission (SMM) (TANDBERG-HANSSEN et al., 1981).

2.2. HANLE effect

Weak coronal magnetic fields cannot be measured by means of the ZEEMAN effect, but here another effect offers an opportunity to determine magnetic fields: Low particle densities n, that means small collisional rates, and the anisotropy of the radiation field favour re-emission by coherent scattering resulting in a net linear polarization in some resonance lines. This resonance fluorescence or HANLE effect is caused by the interference of overlapping magnetic sublevels, therefore the polarization depends on B, on the quantum numbers of lower and upper levels of the transition, and on the geometry of the scattering process. At zero magnetic field the effect does not vanish but results in pure linear polarization similar to RAYLEIGH scattering.

At the Sun the effect shows maximum polarization outside and parallel to the limb, increasing with distance from it. A magnetic field parallel to the limb causes some depolarization and a rotation of the plane of polarization around the magnetic field direction. The conditions to observe the effect are favourable for prominences at the limb, therefore till now successful magnetic field measurements by means of the HANLE effect in the HeI D3 line have been carried out for prominences only (SAHAL-BRÉCHOT et al., 1977; LEROY, 1977). Ultraviolet observations from space will provide very probably HANLE effect measurements in the near future as it has been proposed by STENFLO (1978);

ambiguities in the derivation of the magnetic field structure may be eliminated at least partly by simultaneous observations in different lines (GOPASYUK, 1979).

2.3. Radio emission

Radiation in the visible and near infrared ranges of the solar spectrum are mostly emitted from the deepest layers of the solar atmosphere, the photosphere; electromagnetic waves with larger wavelength, that is radio emission, originate in increasingly higher layers of chromosphere (mm and cm), transition layer (dm) and corona (metre waves). Emission and absorption as well as propagation of radio waves depend not only on density n and temperature T, but also on the magnetic field $\underset{\sim}{B}$, therefore intensity and polarization of the radio emission contain information on $\underset{\sim}{B}$ in the considered regions. Radio observations generally offer the advantage of a high time resolution power which is of great importance for explosive bursts, but it is more difficult to obtain a good resolution in space as compared with observations at shorter wavelengths. This situation will surely be improved in the near future: Large interferometers such as RATAN, VLA, and Westerbork become available also for solar work and yield radio maps with a spatial resolution similar to optical observations at least in the microwave region (KRÜGER, 1979).

For non-burst radio waves the mechanisms of generation (mainly bremsstrahlung from thermal electrons and gyroresonance absorption at large B) and propagation seem to be well known. This enables the construction of complex models for the radio emission, e. g. for the S-component of active regions, including the spatial structure of $\underset{\sim}{B}$, n, and T, the assumptions on which may be tested by comparison of the calculated and observed emissions (GELFREIKH, 1979; BROMBOSZCZ et al., 1981a, b, 1982). Information on coronal magnetic field structure may also be obtained from occultations of external radio sources, e. g. the Crab Nebula or a spacecraft behind the Sun, resulting in FARADAY rotation or in scattering of radio waves at coronal irregularities.

The most intense radio emission originates in bursts in connection with flare events. Its dynamic spectra, that is the intensity or polarization depending on both time and frequency, contain important fine structures which are caused by very different effects such as MHD shock waves, streams of fast electrons or relativistic electrons gyrating about $\underset{\sim}{B}$. Generally speaking the burst radiation contains information on violent magnetic field changes in the flare rather than on the general structure of $\underset{\sim}{B}$ before the flare. The physical mechanisms of burst radiation are far from being well established, providing only order-of-magnitude estimates of B from the observed burst emission with results strongly differing among one another for the different theories under discussion. The situation seems to be most favourable for microwave bursts for which emission models consistent with radio and hard X-ray observations have been proposed (BÖHME et al., 1976, 1977). With increasing wavelength our knowledge of the relevant plasma processes declines, being in need of independent information on $\underset{\sim}{B}$ in order to test the proposed models by comparison with observations.

2.4. Contrast pictures in the visible, UV, and soft X-ray regions of the solar spectrum

Filtergrams taken in selected spectral lines or continuum parts of the solar spectrum often show contrast features which seem to outline the magnetic field structure; the latter conclusion may only be drawn from comparison with polarization measurements which must be consulted for calibration and corroboration. At photospheric level strong magnetic field fine structures such as faculae or supergranular network points appear bright especially in line cores, but larger flux concentrations in pores or sunspots

are dark. With increasing height chromospheric and coronal layers show a pronounced and discrete fine structure which is very probably controlled by magnetic flux concentrations: Outwardly decreasing gas pressure and density in spite of increasing temperature result in a predominance of magnetic pressure and energy, while electric conductivity remains very large parallel to the magnetic field. Plasma motions and all other transport mechanisms such as electric currents, thermal conductivity, and MHD waves are canalized by the magnetic field. If we also take into account the small heat capacity it becomes clear how small variations in heating mechanisms may result in strong local effects. The magnetic field will mainly be force-free (see Section 3.), but small deviations from the force-free structure are sufficient to result in a strong influence of the LORENTZ forces on the plasma.

In the chromosphere the contrast of faculae and supergranular boundaries increases with height, sunspots become brighter. Generally speaking chromospheric longitudinal magnetic fields appear bright in the lines Hα, CaII H and K, MgII h and k, and in EUV lines, while Hα fibrils indicate the direction of the transverse fields. In the corona closed magnetic fields appear as loops of very different lengths mainly in EUV and X-ray lines, while large-scale structures of open diverging lines of force are visible as dark coronal holes. Also other structures such as prominences and coronal streamers are connected with special magnetic field structures, probably with current sheets.

The contrast pictures look quite different in the separate lines caused by the diverse mechanisms of line formation and radiative transfer. For instance, collisionally controlled lines such as CaII H and K are mainly determined by local values of T and n, the latter for their part being determined by the magnetic field at higher levels of the atmosphere. The situation is more complicated for lines which are mainly controlled by the external radiation field: Generally speaking the problem becomes non-local, but Hα filtergrams - the most important contrast pictures till now available - clearly show the local influence of $\underset{\sim}{B}$ on the line contour. This may be due to different effects: The profile of the line absorption coefficient may be modified by plasma streams and by changes of thermal and non-thermal turbulence in the magnetic field. This will result in changes of the source function and therefore of the scattering term, but also frequency-dependent changes of the optical depth scale are possible. The latter may also be due to a modified number of absorbing atoms in the considered feature (GEBBIE and STEINITZ, 1973; STEINITZ et al., 1977). In any case line-of-sight integration effects in the inhomogeneous medium render much more difficult to localize the features in the solar atmosphere, but this also relates to other observations such as polarization measurements. The problem may be partly solved by combination of disk and limb observations and again by simultaneous observations in different lines.

3. Determination of the magnetic field in the chromosphere and in the corona on the base of photospheric magnetograms

3.1. Introduction; force-free character of the magnetic field

Since reliable magnetic field measurements are restricted to the photospheric level, it appears reasonable to compute the magnetic field in the chromosphere and in the corona from that measured in the photosphere using physically realistic assumptions.

Neglecting displacement currents (magnetohydrodynamic approximation), one has for the magnetic induction $\underset{\sim}{B}$ and the electric current density $\underset{\sim}{j}$:

$$\nabla \times \underset{\sim}{B} = \mu_0 \cdot \underset{\sim}{j} \qquad (3.1)$$

Representing the divergence-free magnetic induction by a divergence-free vector potential $\underset{\sim}{A}$ -

$$\underset{\sim}{B} = \nabla \times \underset{\sim}{A}, \qquad \nabla \cdot A = 0 \tag{3.2}$$

- (3.1) becomes

$$\Delta \underset{\sim}{A} = -\mu_0 \underset{\sim}{j} \tag{3.3}$$

Then the magnetic induction at position $\underset{\sim}{r}$ is given by

$$\underset{\sim}{B}(\underset{\sim}{r}) = \frac{\mu_0}{4\pi} \int \nabla \times \left(\frac{\underset{\sim}{j}(\underset{\sim}{r}')}{|\underset{\sim}{r} - \underset{\sim}{r}'|} \right) dV'. \tag{3.4}$$

Here one can see that for a determination of the magnetic field the current density distribution in all space (all contributing sources) is needed. The magnetic field in the solar atmosphere is generated by both subphotospheric and atmospheric electric currents. Only when the magnetic field in a volume V is exclusively generated by sources outside V, for its determination in V the knowledge of the current density distribution (outside V) can be replaced by information on the magnetic field at the boundary of V: Then,

$$\nabla \times \underset{\sim}{B} = 0 \tag{3.5}$$

in V. $\underset{\sim}{B}$ can be represented by a scalar potential φ.

$$\underset{\sim}{B} = -\nabla \varphi \tag{3.6}$$

which, because of $\nabla \cdot \underset{\sim}{B} = 0$, satisfies the LAPLACE equation

$$\Delta \varphi = 0. \tag{3.7}$$

$\underset{\sim}{B}$ can be determined from its normal component at the boundary of V: A NEUMANN boundary value problem for the LAPLACE equation must be solved. When, however, sources inside V contribute to the generation of the magnetic field the (eventually implicit) knowledge of the current density in V is needed. Therefore, the magnetic field in the solar atmosphere can only then be determined from the photospheric magnetic field measurements (without additional information or assumptions) when it is fully (or to good approximation) generated by subphotospheric or photospheric sources. Surely, the main solar atmospheric magnetic field is caused by subphotospheric and photospheric currents. However, the existence of electric currents in the chromosphere and in the corona is very likely. Many activity phenomena seem to be connected with magnetic field structures containing extractable energy and with changes in these configurations. For example, it is widely accepted that flares are caused by a release of stored magnetic energy. Since the subphotospheric currents are assumed not to be influenced by flares, atmospheric currents must exist as source of the flare energy.

Under the condition that the magnetic pressure exceeds the gas pressure appreciably, which prevails in the solar atmosphere (STURROCK and WOODBURY, 1967), the LORENTZ force $\underset{\sim}{j} \times \underset{\sim}{B}$ should lead to strong material acceleration. But in active regions such accelerations are exceptional (flares); over extended time periods the development seems to be quasisteady. As a consequence, if appreciable currents are present, these must be aligned with the magnetic field, since otherwise the resulting LORENTZ force could not be balanced by nonmagnetic forces. Therefore,

$$\underset{\sim}{j} \times \underset{\sim}{B} = 0 \tag{3.8}$$

or, because of (3.1),

$$\nabla \times \underset{\sim}{B} = \alpha \underset{\sim}{B}. \tag{3.9}$$

The factor α is in general a function of position and time. $\alpha = 0$ corresponds to the potential field.

By taking the divergence of (3.9) it follows (taking into account $\nabla \cdot \underset{\sim}{B} = 0$)

$$\nabla \alpha \cdot \underset{\sim}{B} = 0, \tag{3.10}$$

i. e., α is a constant along each magnetic field line or, the field lines lie in the surfaces α = constant. In the case of α = constant, by taking the divergence of (3.9), it is seen that $\nabla \cdot \underset{\sim}{B} = 0$ is automatically satisfied (except for $\alpha = 0$).

α^2 is a measure for that part of the magnetic energy which is transformed into heat by JOULE dissipation (GAIL, 1969): The square of (3.9) is

$$(\nabla \times \underset{\sim}{B})^2 = \alpha^2 \underset{\sim}{B}^2. \tag{3.11}$$

Using (3.1) this becomes

$$\alpha^2 = \frac{\sigma \mu_0}{2} \cdot \frac{\frac{1}{\sigma} \underset{\sim}{j}^2}{\frac{1}{2\mu_0} \underset{\sim}{B}^2}. \tag{3.12}$$

If $\underset{\sim}{t}$ denotes the unit vector in the magnetic field direction, $\underset{\sim}{B} = |\underset{\sim}{B}| \cdot \underset{\sim}{t}$, one gets from (3.9) (cf. BOSTRÖM, 1973)

$$\nabla |\underset{\sim}{B}| \times \underset{\sim}{t} + |\underset{\sim}{B}| \nabla \times \underset{\sim}{t} = \alpha |\underset{\sim}{B}| \underset{\sim}{t} \tag{3.13}$$

and after scalar multiplication with $\underset{\sim}{t}$:

$$\alpha = \underset{\sim}{t} \cdot \nabla \times \underset{\sim}{t}. \tag{3.14}$$

This shows that α is a simple function of the geometry of the field lines. It is a measure for the torsion of neighbouring field lines around each other.

3.2. Practical representation of the magnetic field

Each divergence-free field $\underset{\sim}{B}$,

$$\nabla \cdot \underset{\sim}{B} = 0, \tag{3.15}$$

can be represented as the sum of a toroidal and a poloidal part in the forms

$$\underset{\sim}{B} = \underset{\sim}{r} \times \nabla T_r + \nabla \times (\underset{\sim}{r} \times \nabla P_r), \quad \text{or} \tag{3.16}$$

$$\underset{\sim}{B} = \underset{\sim}{e} \times \nabla T_e + \nabla \times (\underset{\sim}{e} \times \nabla P_e), \tag{3.17}$$

respectively, by scalar function pairs T_r, P_r and T_e, P_e, respectively (CHANDRASEKHAR, 1961, RÄDLER, 1974), $\underset{\sim}{r}$ denoting the radius vector and $\underset{\sim}{e}$ a constant vector.

In representing solar atmospheric magnetic fields, in general, the considered volume is that between two spherical shells (with the exterior of a sphere as a special case) or it is a semi-infinite cylinder above plane base (with the half space as a special case). In the first case the use of (3.16) is adequate, in the latter that of (3.17).

In a system of Cartesian coordinates, x, y, z, consider the representation (3.17) with $\underset{\sim}{e} = (0,0,1)$: The generating functions P_e, T_e are not determined uniquely. The functions

$$\hat{P}_e = P_e + \mathrm{Re}\, f(x + iy, z), \tag{3.18}$$

$$\hat{T}_e = T_e - \mathrm{Im} \frac{\partial}{\partial z} f(x + iy, z) \tag{3.19}$$

- $f(x + iy, z)$ is an analytic function of $(x + iy)$ with arbitrary z-dependence-generate, according to (3.17), the same divergence-free field. (There are no further generating function pairs than those given by (3.18, 3.19) (NAKAGAWA and RAADU, 1972)).

For α = const. (in (3.9)), using (3.17), one gets

$$\underset{\sim}{e} \times \nabla (\alpha T_e + \Delta P_e) + \nabla \times (\underset{\sim}{e} \times \nabla (\alpha P_e - T_e)) = 0. \tag{3.20}$$

Hence,

$$\alpha P_e - T_e = \mathrm{Re}\, f(x + iy, z) \tag{3.21}$$

and

$$\alpha T_e + \Delta P_e = - \frac{\partial}{\partial z} \mathrm{Im}\, f(x + iy, z) \tag{3.22}$$

(cf. NAKAGAWA and RAADU, 1972). One can show (SEEHAFER, 1979, p. 55) that the choice $f = 0$ is possible without loss of generality. Then it follows that a constant-α force-free magnetic field can be represented in the form

$$\underset{\sim}{B} = \alpha \underset{\sim}{e} \times \nabla P + \nabla \times (\underset{\sim}{e} \times \nabla P) \tag{3.23}$$

by a solution P of the scalar HELMHOLTZ equation

$$\Delta P + \alpha^2 P = 0. \tag{3.24}$$

The possibility of the analogous representation

$$\underset{\sim}{B} = \alpha \underset{\sim}{r} \times \nabla P_r + \nabla \times (\underset{\sim}{r} \times \nabla P_r) \tag{3.25}$$

by a solution P_r of the HELMHOLTZ equation has, for example, been shown by RÄDLER (1974).

For $\alpha \neq$ const. such a reduction of the equations (3.9), (3.15) to one single partial differential equation for one scalar function is not possible.

The solutions P and P_r, respectively, of the HELMHOLTZ equation which generate $\underset{\sim}{B}$ according to (3.23) and (3.25), respectively, are, also, not unique. For $\underset{\sim}{B} = 0$ (3.23), for example, has the general solution

$$P_0(x, y, z) = \mathrm{Re}\,[f(x + iy)] \cos \alpha z + \mathrm{Im}\,[f(x + iy)] \sin \alpha z \tag{3.26}$$

(SEEHAFER, 1979, p. 55).

For the case that the considered volume extends to infinity in the z direction, from this one can see that there can be only one generating function P vanishing as $z \to \infty$. In this case, from the vanishing of $\underset{\sim}{B}$ at infinity it follows that there is, in fact, one and only one generating function P vanishing as $z \to \infty$ (SEEHAFER, 1979, p. 60).

If the planes of intersection z = const. through the considered volume occupy the whole x-y plane (as in the case of the half space $z = 0$), the general form (3.26) of the function P_0 generating the field $\underset{\sim}{B} = 0$ is reduced to

$$P_0(x, y, z) = C_1 \cos \alpha z + C_2 \sin \alpha z, \tag{3.27}$$

C_1 und C_2 being arbitrary constants, since there is no function which is analytic in the whole complex plane and which is not a constant.

Similarly, the fact that a function F which satisfies the equation

$$\frac{1}{\sin\theta}\frac{\partial}{\partial\theta}\left(\sin\theta\,\frac{\partial F}{\partial\theta}\right)+\frac{1}{\sin^2\theta}\frac{\partial^2 F}{\partial\phi^2}=0 \qquad (3.28)$$

(the operator on the left-hand side is the θ-ϕ part of the Laplacian) on a whole spherical surface must be a constant reduces the arbitrariness in chosing the generating functions P_r and T_r of the representations (3.16) and (3.25) - of interest when the volume between two spherical surfaces is considered. The functions P_r and T_r of the representation (3.16) of a divergence-free field are then each determined except for an arbitrary function of r ($= |\underset{\sim}{r}|$) (RÄDLER, 1974). Analogously to (3.27), the function P_r generating a force-free magnetic field with α = const. according to (3.27) is determined except for a function of the form

$$P_{ro} = C_1 \frac{1}{\sqrt{r}} H^{(1)}_{1/2}(\alpha r) + C_2 \frac{1}{\sqrt{r}} H^{(2)}_{1/2}(\alpha r), \qquad (3.29)$$

where $H^{(1)}_{1/2}$ and $H^{(2)}_{1/2}$ denote the HANKEL functions of the first and second kind, respectively, of the order 1/2. P_{ro} vanishes as $r \to \infty$; the requirement of vanishing at infinity is not sufficient for the generating function to be determined uniquely (there remain two arbitrary constants). On the other hand, also here, the existence of a generating function vanishing as $r \to \infty$ can be shown.

3.2.1. Start from magnetograms of the whole photosphere

3.2.1.1. Potential field

An extensively applied method to calculate a current-free magnetic field in the solar atmosphere is based on the source-surface model introduced by SCHATTEN et al. (1969) (first) and, together with a more powerful computational technique, by ALTSCHULER and NEWKIRK (1969). The current-free magnetic field in the volume between the photosphere and a surface at some radial distance R_w (about 2.5 $R_\odot$) is computed. The assumption that the field becomes radial, thereby simulating the effects of the solar wind, provides the boundary condition at $r = R_w$.

In the region where no electric currents flow, the magnetic field can be derived according to (3.6) from a scalar potential φ satisfying the LAPLACE equation (3.7).

In a system of spherical coordinates, r, θ, ϕ, (origin at the centre of the Sun), the potential between the two spherical surfaces at $r = R$ and $r = R_w$ is given by (CHAPMAN and BARTELS, 1940, p. 625)

$$\varphi(r,\theta,\phi) = R_\odot \sum_{n=1}^{\infty}\sum_{m=0}^{n} P^m_n(\mu)\left\{\left[c^m_n\left(\frac{r}{R_\odot}\right)^n + (1-c^m_n)\left(\frac{R_\odot}{r}\right)^{n+1}\right] g^m_n \cos m\phi + \right.$$

$$\left. + \left[d^m_n\left(\frac{r}{R_\odot}\right)^n + (1-d^m_n)\left(\frac{R_\odot}{r}\right)^{n+1}\right] h^m_n \sin m\phi\right\}. \qquad (3.30)$$

$P^m_n(\mu)$ are the associated LEGENDRE functions of the degree n, the order m, and the argument $\mu = \cos\theta$, while c^m_n, d^m_n, g^m_n, and h^m_n denote constants.

With $c^m_n = d^m_n = 0$ the right-hand side of (3.30) takes the form of the solution of the LAPLACE equation in the volume $r \geq R_\odot$ which vanishes as $r \to \infty$.

The requirement that the field becomes radial at $r = R_w$ is satisfied if $r = R_w$ is a zero-potential surface,

$$(R_w, \theta, \phi) = 0, \qquad (3.31)$$

this condition being satisfied by

$$o_n^m = d_n^m = -\left[(R_w/R_\odot)^{2n+1} - 1\right]^{-1} \tag{3.32}$$

(ALTSCHULER and NEWKIRK, 1969).

The remaining coefficients h_n^m, g_n^m must be determined from photospheric magnetic field measurements. This requires data collection over a complete solar rotation. Since the reliability of the magnetic field measurements (measurements of the component parallel to the line of sight) decreases with increasing distance from disk center, the field is measured for each area element as it passes central meridian. In principle, by additionally using measurements before and/or after central meridian passage, the magnetic field components in two different directions, both lying in the ecliptic plane, could be determined, i. e., besides the line-of-sight component,

$$B_\parallel = B_r \cdot \sin\theta + B_\theta \cdot \cos\theta, \tag{3.33}$$

also the azimuthal component B_ϕ. Instead of this, because of too strong variations from day to day and in order to record only the persistent magnetic features (according to the data collection over a period of 28 days), measurements of several days as an area element passes central meridian are averaged (ALTSCHULER et al., 1977).

ALTSCHULER and NEWKIRK (1969) determine the coefficients g_n^m, h_n^m by minimizing the difference between measured and computed line-of-sight component using a least mean square fit procedure. RIESEBIETER and NEUBAUER (1979) have shown that they can be determined directly by using the orthogonality relation of the spherical harmonics.

The magnetic field can also be obtained without the use of spherical harmonics. ADAMS and PNEUMAN (1976) have described a fixed mesh method for solving the LAPLACE equation. They convert the non-standard boundary condition $B_\parallel$ to a DIRICHLET boundary condition.

A modification of the source-surface model was proposed by SCHULZ et al. (1978). They use a non-spherical source surface, which is taken to be an isogauss of the underlying potential field generated by currents in or below the photosphere, i. e., an isogauss of the magnetic field that is current-free in the volume $r > R_\odot$ and satisfies the photospheric boundary condition. In this way they get a better agreement with an exact MHD solution calculated by PNEUMAN and KOPP (1971) for the case that the normal component of the photospheric magnetic field is that of a dipole.

A more direct modeling, in comparison with the source-surface model, of the coupling between the magnetic field and the plasma was developed by YEH and PNEUMAN (1977). The volume above the photosphere is partitioned into several piecewise current-free regions separated by current sheets. Starting from an initial magnetic field configuration (e. g. a source-surface solution) the current-sheets are placed between closed and open field lines and between oppositely directed open field lines. Then the imbalance between magnetic and plasma pressures across the current-sheets is computed and used as a guide for a displacement of the current sheets. The desired solution is obtained by iteration between the computation of the magnetic field in the current-free regions and the displacement of the partitioning surfaces. Also for this solution, the agreement with the MHD dipole solution of PNEUMAN and KOPP (1971) is reported to be better than for the spherical source-surface solution.

Using the measurements of modern magnetographs, which supply high resolution ($\approx 1''$) magnetograms of the full solar disk, the magnetic field extrapolation starting from global magnetograms provides a method not only for representing the large-scale magnetic field but also for a detailed mapping of the magnetic field above any small photospheric region (ALTSCHULER et al., 1977), provided these small-scale structures are long-lived enough.

3.2.1.2. Force-free magnetic field with α = const. ($\neq 0$)

In the case of the force-free magnetic field with α = const. instead of the LAPLACE equation the HELMHOLTZ equation (3.24) (the LAPLACE equation is the special form of the HELMHOLTZ equation for $\alpha = 0$) must be solved. There are some differences between the LAPLACE equation and the HELMHOLTZ equation (SEEHAFER, 1978): If a solution of the LAPLACE equation vanishes at the boundary surface S of a finite region and at infinity, it vanishes identically outside S, while under similar conditions a solution of the HELMHOLTZ equation does not necessarily vanish (cf. MÖLLER, 1969). For example,

$$f_1 (\underset{\sim}{r}) = \frac{\sin \alpha r}{r} \tag{3.34}$$

and

$$f_2 (\underset{\sim}{r}) = \frac{\cos \alpha r}{r} \tag{3.35}$$

are solutions of the HELMHOLTZ equation that vanish at infinity. One can always find a linear combination of f_1 and f_2 that vanishes at some distance $r = R$ (and at infinity).

An exterior boundary value problem with a unique solution can be posed by means of an extra condition at infinity (MÖLLER, 1969), namely the SOMMERFELD radiation condition

$$P = o (r^{-1}), \qquad \frac{\partial P}{\partial r} + i \alpha P = o (r^{-1}). \tag{3.36}$$

Let uns consider the exterior boundary value problem for the sphere in detail. P can be represented by a harmonic expansion

$$P (r, \theta, \phi) = \sum_{n=0}^{\infty} \sum_{j=-n}^{n} R_{nj} (r) Y_n^{(j)} (\theta, \phi), \tag{3.37}$$

where $Y_n^{(j)}$ denote spherical harmonics of degree n and order j. Then, the coefficients $R_{nj} (r)$ must satisfy the equation

$$R''_{nj} + \frac{2}{r} R'_{nj} + (\alpha^2 - \frac{n (n + 2)}{r^2}) R_{nj} = 0. \tag{3.38}$$

The general solution of (3.38)can be written in form

$$R_{nj} (r) = A_{nj} \frac{1}{\sqrt{r}} H^{(1)}_{n+1/2} (\alpha r) + B_{nj} \frac{1}{\sqrt{r}} H^{(2)}_{n+1/2} (\alpha r), \tag{3.39}$$

where $H^{(1)}_{n+1/2}$ and $H^{(2)}_{n+1/2}$ denote the HANKEL functions of the first and second kind, respectively, of the order $n + 1/2$, and A_{nj}, B_{nj} are arbitrary constants. One can see that the general solution $R_{nj} (r)$ vanishes as $r \to \infty$. None of the constants can be determined from the requirement of $R_{nj} (r)$ vanishing at infinity. Clearly, if only one magnetic field component is given at $r = R_\odot$ (photosphere), it is impossible to determine both A_{nj} and B_{nj}. NAKAGAWA (1973) gives a solution of the boundary value problem with only one set of constants to be determined. Obviously, he does not use the general solution (3.39) of (3.38) although (implicitly) claiming to do this.

To define a unique boundary value problem an additional condition is needed. The SOMMERFELD radiation condition (3.36), which is used in studying wave propagation, is not adequate to the problem. An adequate condition would be that the magnetic field outside the Sun had a finite energy content.

The magnetic energy content M within the volume of analysis is given by

$$M = \frac{1}{2\mu_o} \int_V |\underset{\sim}{B}|^2 \, dV. \tag{3.40}$$

From the representations (3.23) and (3.25), it can easily be verified that not only the generating functions P and P_r but also the magnetic field components B_x, B_y, B_z, and B_r satisfy the HELMHOLTZ equation. Now one can show (RELLICH, 1943, see also MÖLLER, 1969), that, if u is a function that satisfies the HELMHOLTZ equation (3.24) with $\alpha \neq 0$ for $r > R$, the function

$$f(R_1) = \int_{R<r<R_1} |u|^2 \, dV \tag{3.41}$$

tends to infinity as $R_1 \to \infty$. Thus, we have the remarkable result that a magnetic field being force-free with α = constant everywhere outside the Sun cannot have a finite energy content (except for $\alpha = 0$). Therefore the use of global-scale constant-α force-free magnetic fields must be confined to the consideration of finite volumes. A generalization of the source-surface model to cases of $\alpha \neq 0$ seems reasonable. However, a force-free magnetic field which is not current-free cannot be perpendicular to a (regular) surface on this surface. In the case of the sphere this is immediately seen since the curl of a radial field has no radial component: For a radially directed field $\underset{\sim}{B}$, it is $\nabla \times \underset{\sim}{B} \perp \underset{\sim}{B}$, whereas for a force-free field $\nabla \times \underset{\sim}{B} \parallel \underset{\sim}{B}$ holds. Now let the source-surface be arbitrarily formed and given by

$$F(\underset{\sim}{r}) = 0. \tag{3.42}$$

A field $\underset{\sim}{B}$ normal to this surface can be represented by

$$\underset{\sim}{B} = f(\underset{\sim}{r}) \, \nabla F(\underset{\sim}{r}), \tag{3.43}$$

with f being an arbitrary function of $\underset{\sim}{r}$. Then, from (3.14) it follows

$$\alpha = \frac{f}{B} \nabla F \cdot \nabla \times \left(\frac{f}{B} \nabla F\right) = \frac{f}{B} \nabla F \cdot \left(\nabla \frac{f}{B} \times \nabla F\right) = 0. \tag{3.44}$$

That is to say, the magnetic field must be current-free. A generalization of the source-surface model to cases of $\alpha \neq 0$ must also contain a generalization of the way of matching to the outer solar wind dominated regions. BARBOSA (1978a) proposed to determine the constant-α force-free magnetic field between two concentric spheres by prescribing (in addition to the photospheric boundary condition) the values of B_r on the outer surface. At the present time, however, there is no possibility to get this latter information from measurements.

3.2.2. Start from magnetograms of limited photospheric regions

If one determines current-free or constant-α force-free magnetic fields from magnetograms of limited photospheric regions the data are not sufficient to define a unique boundary value problem. The possible influence of magnetic fields surrounding the magnetogram area must be referenced to in terms of special assumptions (additional boundary conditions).

3.2.2.1. Extrapolation procedures assuming flux balance over the magnetogram area

There are two extensively applied extrapolation procedures that start from magnetograms of limited photospheric regions and require the net magnetic flux through the magnetogram area to be zero, the procedures of SCHMIDT (1964) and of NAKAGAWA and RAADU (1972).

The SCHMIDT procedure assumes the magnetic field to be current-free. A NEUMANN boundary value problem for the LAPLACE equation for a half space is solved, assuming that the magnetic field component normal to the boundary plane vanishes everywhere on this plane outside the region covered by the magnetogram. There it is given by the magnetogram. The magnetic field is represented in the form (3.6) as the negative gradient of a solution φ of the LAPLACE equation in the half space, which may be expressed as the potential of a double layer in the form (SCHMIDT, 1964)

$$\varphi(r) = \frac{1}{2\pi} \int \frac{B}{|\underset{\sim}{r} - \underset{\sim}{r}'|} \, d\sigma_{\underset{\sim}{r}}, \tag{3.45}$$

where the integral is taken over the plane of magnetograph observation.

NAKAGAWA and RAADU (1972) introduced a procedure to compute the constant-α force-free magnetic field in the semi-infinite column above a rectangular photospheric region. For the domain of analysis defined by

$$0 \leq x \leq L_x, \qquad 0 \leq y \leq L_y, \qquad 0 \leq z < \infty, \tag{3.46}$$

they gave the solution P of the HELMHOLTZ equation (3.24) which generates the magnetic field according to (3.23) in the form

$$P = \sum_{k \neq 0} \frac{1}{k^2} B_{\underset{\sim}{k}} \, e^{i \underset{\sim}{k} \underset{\sim}{x} - (k^2 - \alpha^2)^{1/2} z}, \tag{3.47}$$

where $\underset{\sim}{k} = (k_x, k_y)$, $\underset{\sim}{x} = (x, y)$, and the $B_{\underset{\sim}{k}}$ are determined from the photospheric boundary condition,

$$B_z(x, y, z = 0) = \sum_{\underset{\sim}{k}} B_{\underset{\sim}{k}} \, e^{i \underset{\sim}{k} \underset{\sim}{x}}. \tag{3.48}$$

Implicitly, beside the requirement of $B_{00} = 0$, it is required (SEEHAFER, 1975)

$$P(L_x, y, z) = P(0, y, z), \qquad P(x, L_y, z = P(x, 0, z) \tag{3.49}$$

and

$$\left.\frac{\partial P(x, y, z)}{\partial x}\right|_{x=L_x} = \left.\frac{\partial P(x, y, z)}{\partial x}\right|_{x=0},$$

$$\left.\frac{\partial P(x, y, z)}{\partial y}\right|_{y=L_y} = \left.\frac{\partial P(x, y, z)}{\partial y}\right|_{y=0}. \tag{3.50}$$

(3.49) and (3.50) hold also for the magnetic field components B_x, B_y, B_z. That is to say, the field can be two-dimensionally periodically extrapolated into the whole half space.

BARBOSA (1978b) gave a method to compute the constant-α force-free magnetic field in the volume between two parallel planes, the photospheric plane and an additional plane at arbitrary height. The magnetic field component normal to the second plane is assumed to be zero. Again, for applications to magnetograph data, flux balance over the magnetogram area is required.

A further flux balance requiring potential-field solution was given by TEUBER et al. (1977). They assume the normal field component to vanish at the vertical boundary of the rectangular cylinder above the magnetogram area.

Contrary to the other extrapolation procedures mentioned in this section, for that of SCHMIDT flux balance over the magnetogram area is not explicitly required. Indeed, this procedure is mathematically applicable also to cases of flux imbalance. Then the magnetic field vanishes at infinity only as r^{-2} (r denoting the distance from an origin), and the net flux through the magnetogram area is connected to infinity (the magnetic flux

through an infinitely distant half sphere above the photospheric plane is not zero, but equal to the total flux through the magnetogram area). This, however, is an unphysical feature. The procedure must be considered as an approximate (curvature-neglecting) calculation of a potential field exterior to a spherical photosphere. If such a field is represented by a spherical-harmonic expansion, for div $\underset{\sim}{B} = 0$ to be satisfied the zero-order (monopole) term must be excluded. This means that the field vanishes at infinity at least as r^{-3}. Therefore in applying the SCHMIDT procedure the net flux through the magnetogram area must be neglected.

In order to allow for an application to regions which are not close to the center of the solar disk, the SCHMIDT procedure (SEMEL, 1967; SAKURAI, 1982) and the NAKAGAWA-RAADU procedure (WELLCK and NAKAGAWA, 1983) have been generalized such that they start from an oblique line-of-sight component.

3.2.2.2. GREEN's function method for a semi-infinite column

Let the domain of analysis again be given by (3.46) and $z = 0$ define the plane of magnetograph observation. The GREEN's function of the HELMHOLTZ equation in the considered volume is given by (SEEHAFER, 1978)

$$G(\underset{\sim}{r}, \underset{\sim}{r}') = \sum_{m,n=1}^{\infty} \frac{\psi_{mn}(x, y)\psi_{mn}(x', y')}{2r_{mn}} \cdot \left\{ e^{-r_{mn}|z-z'|} - e^{-r_{mn}|z+z'|} \right\} . \quad (3.51)$$

$\psi_{mn}(x, y)$ denote the normalized eigenfunctions of the two-dimensional Laplacian $\Delta_\perp$ in the region $0 \leq x \leq L_x$, $0 \leq y \leq L_y$, i. e. the solutions of the equation

$$\Delta_\perp \psi_{mn} + \lambda_{mn}\psi_{mn} = 0. \quad (3.52)$$

They are given by

$$\psi_{mn}(x, y) = \sqrt{\frac{4}{L_x L_y}} \sin\left(\frac{\pi m}{L_x} x\right) \sin\left(\frac{\pi n}{L_y} y\right). \quad (3.53)$$

The corresponding eigenvalues are

$$\lambda_{mn} = \pi^2 \left(\frac{m^2}{L_x^2} + \frac{n^2}{L_y^2}\right), \quad (3.54)$$

and

$$r_{mn} = \sqrt{\lambda_{mn} - \alpha^2}. \quad (3.55)$$

If the semi-infinite column has another (not rectangular) cross section, the ψ_{mn} must be replaced by the eigenfunctions of the two-dimensional Laplacian in a region of corresponding form. For example, considering a semi-infinite circular cylinder BESSEL functions must be used.

By means of the GREEN's function the values of any solution P of the HELMHOLTZ equation can be obtained from the values of P at the boundary S of the considered volume via the representation

$$P(\underset{\sim}{r}') = -\int_S P(\underset{\sim}{r}) \frac{\partial G}{\partial n} \, dS, \quad (3.56)$$

where $\underset{\sim}{n}$ denotes the exterior normal on S.

The practical use of the GREEN's function representation in applying special boundary conditions has been illustrated by deriving an extrapolation procedure which does not require the net magnetic flux through the magnetogram area to be zero (SEEHAFER, 1978):

To define a unique boundary value problem it is assumed that B_z vanishes on the vertical part of the boundary, at $x = 0$, $x = L_x$, $y = 0$, $y = L_y$ (that the values of B_z at the boundary are small compared with its values at the inner parts of the cross section of the column). Then the magnetic field components are obtained in the forms

$$B_x = \sum_{m,n=1}^{\infty} \frac{C_{mn}}{\lambda_{mn}} e^{-r_{mn}z} \left\{ \alpha \frac{\pi n}{L_y} \sin\left(\frac{\pi mx}{L_x}\right) \cos\left(\frac{\pi ny}{L_y}\right) - \right.$$

$$\left. - r_{mn} \frac{\pi m}{L_x} \cos\left(\frac{\pi mx}{L_x}\right) \sin\left(\frac{\pi ny}{L_y}\right) \right\}, \qquad (3.57a)$$

$$B_y = -\sum_{m,n=1}^{\infty} \frac{C_{mn}}{\lambda_{mn}} e^{-r_{mn}z} \left\{ \alpha \frac{\pi m}{L_x} \cos\left(\frac{\pi mx}{L_x}\right) \sin\left(\frac{\pi ny}{L_y}\right) + \right.$$

$$\left. + r_{mn} \frac{\pi n}{L_y} \sin\left(\frac{\pi mx}{L_x}\right) \cos\left(\frac{\pi ny}{L_y}\right) \right\}, \qquad (3.57b)$$

$$B_z = \sum_{m,n=1}^{\infty} C_{mn} e^{-r_{mn}z} \sin\left(\frac{\pi mx}{L_x}\right) \sin\left(\frac{\pi ny}{L_y}\right), \qquad (3.57c)$$

where the C_{mn} are defined by the expansion (3.57c) at $z = 0$. (For the practical application the magnetogram must be changed or completed such that the values at the boundary vanish, for example by adding an artificial boundary.)

There is a close similarity between the representation (3.57) and the representation (3.47) of NAKAGAWA and RAADU (1972). The solution (3.57) is periodic, as the solution of NAKAGAWA and RAADU, but with the periods $2L_x$ and $2L_y$, whereas the solution of NAKAGAWA and RAADU has the periods L_x and L_y. One can get the solution (3.57) by extrapolating the magnetogram, which covers the domain $0 \leq x \leq L_x$, $0 \leq y \leq L_y$, into the domain $-L_x \leq x \leq L_x$, $-L_y \leq y \leq L_y$ according to

$$B_z(-x, y, 0) = -B_z(x, y, 0), \qquad (3.58)$$

$$B_z(x, -y, 0) = -B_z(x, y, 0), \qquad (3.59)$$

and then applying the formulae of NAKAGAWA and RAADU to the extrapolated magnetogram. The solution of NAKAGAWA and RAADU is got in the same way if the extrapolation of the magnetogram into the domain $-L_x \leq x \leq 0_x$, $-L_y \leq y \leq L_y$ is carried out according to

$$B_z(-x, y, 0) = B_z(x, y, 0), \qquad (3.60)$$

$$B_z(x, -y, 0) = B_z(x, y, 0). \qquad (3.61)$$

The use of (3.58) and (3.59) instead of (3.60) and (3.61) ensures that the net magnetic flux through the (original) magnetogram area is balanced.

As to the conditions on the (vertical part of the) boundary corresponding to the two solutions, the solution (3.57) seems more restrictive in that it requires the vertical magnetic field component to vanish at the boundary, whereas (3.47) only requires that (3.49) is fulfilled. However, (3.47) requires additionally (3.50), which the solution (3.57) does not.

For an application of (3.57) at first the coefficients C_{mn} must be determined from the magnetogram. Since B_z is represented by an expansion in orthogonal functions, for regions close to the disk center, that is, in cases with $B_z(x, y, z = 0)$ given this is easily done by integrations. Now let the direction to the observer be defined by the unit vector $\underset{\sim}{l} = (l_x, l_y, l_z)$. According to (3.57) the line-of-sight component provided by the magnetogram is then given by

$$B_{\parallel} = \underset{\sim}{B} \cdot \underset{\sim}{l} = \sum_{m,n=1}^{\infty} C_{mn} \varphi_{mn} \tag{3.62}$$

with

$$\varphi_{mn} = \sin\left(\frac{\pi m x}{L_x}\right) \cos\left(\frac{\pi n y}{L_y}\right) \cdot \frac{\pi n}{L_y \lambda_{mn}} (l_x \alpha - l_y r_{mn}) + \tag{3.63}$$

$$+ \cos\left(\frac{\pi m x}{L_x}\right) \sin\left(\frac{\pi n y}{L_y}\right) \cdot \frac{\pi m}{L_x \lambda_{mn}} (-l_x r_{mn} - l_y \alpha) + \sin\left(\frac{\pi m x}{L_x}\right) \sin\left(\frac{\pi n y}{L_y}\right) \cdot l_z .$$

The C_{mn} are the coefficients of the expansion of $B_{\parallel}$ in the function system φ_{mn}. Compared with the determination of the corresponding coefficients of the NAKAGAWA-RAADU solution from an oblique line-of-sight component (WELLCK and NAKAGAWA, 1973), their determination is complicated by the fact that the function system φ_{mn} is not orthogonal on the interval

$$0 \leq x \leq L_x, \qquad 0 \leq y \leq L_y .$$

One may proceed such that first the coefficients K_{mn} of the expansion

$$B_{\parallel} = \sum_{m,n=1}^{\infty} K_{mn} \psi_{mn} \tag{3.64}$$

of $B_{\parallel}$ in the orthogonal functions ψ_{mn} given by (3.53) are determined. The matrix T_{kl}^{mn} describing the transformation from the system ψ_{mn} to the system φ_{mn} according to

$$C_{kl} = \sum_{m,n=1}^{\infty} T_{kl}^{mn} K_{mn} \tag{3.65}$$

is defined by the expansions

$$\psi_{mn} = \sum_{k,l=1}^{\infty} T_{kl}^{mn} \varphi_{kl} . \tag{3.66}$$

That is, the elements T_{kl}^{mn} are coefficients of expansions in the non-orthogonal functions φ_{kl}. This is not the case for the inverse matrix

$$U_{kl}^{mn} = (T_{kl}^{mn})^{-1}, \tag{3.67}$$

which is defined by the expansions (in orthogonal functions)

$$\varphi_{mn} = \sum_{k,l=1}^{\infty} U_{kl}^{mn} \psi_{kl} \tag{3.68}$$

and provides for the transformation

$$K_{kl} = \sum_{m,n=1}^{\infty} U_{kl}^{mn} C_{mn} . \tag{3.69}$$

Therefore, after determining the K_{mn} according to (3.64) and the U_{kl}^{mn} according to (3.68), one can get the T_{kl}^{mn} by matrix inversion according to (3.67) and, finally, the C_{kl} by matrix multiplication according to (3.65). In this way the problem of data conversion is reduced to a matrix inversion, for which efficient computer programs are available.

The solution (3.57) has already been applied in order to extrapolate magnetograms from active regions of August 3 and 7, 1972 (SEEHAFER and STAUDE, 1977, 1979), of July 4, 1973 (SEEHAFER and STAUDE, 1980; see Section 4.), and of July 8 to 11, 1975 (SEEHAFER, 1980).

3.2.2.3. Determination of the magnetic field as CAUCHY problem: Vertical integration scheme

It seems desirable to determine the magnetic field from photospheric measurements alone, without additional assumptions ("boundary conditions"). The extrapolation of measured photospheric magnetic fields to higher layers of the solar atmosphere is originally not a boundary value problem but an initial value problem: Data are given on an initial surface which is not the complete enclosure of the considered volume. Boundary value problems are formulated because these are "natural" for the partial differential equations to be solved, which are, for force-free magnetic fields, of elliptic type. For a determination of the magnetic field without imposing conditions on the non-photospheric part of the boundary, the corresponding information should be contained in additional photospheric data. Such data can become available by the improvement of vector magnetographs (maybe also if these do not in fact supply the full vector). Another possibility may be simultaneous magnetic field measurements in several spectrum lines which are formed at different photospheric levels. In such a way, at least in principle, magnetic field gradients can be obtained.

If the line-of-sight component of the magnetic field and the line-of-sight derivate of this component are given at the level of the photosphere, a CAUCHY problem arises. For a constant-α force-free magnetic field this CAUCHY problem has a unique solution (SEEHAFER 1979, p. 31): A solution P of the HELMHOLTZ equation (3.24) can be represented in the form

$$P = \hat{P} + \hat{\hat{P}} \tag{3.70}$$

with

$$\hat{P}(x, y, z) = \sum_{n=0}^{\infty} (-1)^n (\alpha^2 + \Delta_\perp)^n f(x, y) \frac{z^{2n}}{(2n)!} \tag{3.71}$$

and

$$\hat{\hat{P}}(x, y, z) = \sum_{n=0}^{\infty} (-1)^n (\alpha^2 + \Delta_\perp)^n g(x, y) \frac{z^{2n+1}}{(2n+1)!}, \tag{3.72}$$

where

$$f(x, y) = P(x, y, z = 0), \tag{3.73}$$

$$g(x, y) = \left.\frac{\partial P}{\partial z}\right|_{n=0} \tag{3.74}$$

and

$$\Delta_\perp = \frac{\partial^2}{\partial x^2} + \frac{\partial^2}{\partial y^2}. \tag{3.75}$$

Both $\hat{P}$ and $\hat{\hat{P}}$ are solutions of the HELMHOLTZ equation. At $z = 0$ $\hat{P}$ takes prescribed values $f(x, y)$, whereas its z derivative vanishes there. $\hat{\hat{P}}$ vanishes at $z = 0$, whereas its z derivative takes prescribed values $g(x, y)$.

However, the CAUCHY problem for an elliptic equation is non-well posed, that is to say, the solutions do not depend continuously on the data. Consider, for example, the following sequence of initial values:

$$P_{mn}(x, y, z = 0) = f_{mn}(x, y) = \frac{1}{r_{mn}} \sin\left(\frac{\pi mx}{L_x}\right) \sin\left(\frac{\pi ny}{L_y}\right), \tag{3.76}$$

$$\left.\frac{\partial P_{mn}(x, y, z)}{\partial z}\right|_{z=0} = g_{mn}(x, y) \equiv 0 \tag{3.77}$$

with

$$r_{mn} = \sqrt{\pi^2 \left(\frac{m^2}{L_x^2} + \frac{n^2}{L_y^2}\right) - \alpha^2}\ .$$

According to (3.70), (3.71), and (3.72), the corresponding solutions of the HELMHOLTZ equation are (SEEHAFER, 1979, p. 67)

$$P_{mn}(x, y, z) = \frac{1}{r_{mn}} \cosh(r_{mn} z) \sin\left(\frac{\pi m x}{L_x}\right) \sin\left(\frac{\pi n y}{L_y}\right). \qquad (3.78)$$

As $(m^2 + n^2) \to \infty$, $f_{mn}(x, y)$ tends identically to zero, whereas $P_{mn}(x, y, z)$ does not.

Until recently, mathematicians ignored non-well posed problems. Even today these problems are largely unsettled. However, various methods have been employed for handling such problems (LAVRENTIEV, 1967, Conference proceedings edited by KNOPS, 1973, and by ANGER, 1979). For example, in many cases restriction to the class of solutions satisfying a prescribed global bound leads to well posed problems. Based on this concept, in particular for the LAPLACE equation methods of solution have been developed, which could allow a generalization to the HELMHOLTZ equation. Here it shall only be pointed to this possibility to attack the problem of magnetic field extrapolation. Until now, the data required are not available. However, they will become available. If the full magnetic vector is measured, a CAUCHY problem for the system

$$\nabla \cdot \underset{\sim}{B} = 0, \qquad (\nabla \times \underset{\sim}{B}) \times \underset{\sim}{B} = 0 \qquad (3.79)$$

of quasilinear first-order partial differential equations, which describes the general force-free magnetic field with non-constant α, arises.

4. Application of different extrapolation procedures to the same magnetogram

In order to study the influence of the different treatment of the boundary conditions in different extrapolation schemes, the procedures of SCHMIDT (1964, in the following referred to as SCHP) (Equation (3.45)), of NAKAGAWA and RAADU (1972, referred to as NRP) (Equations (3.47) and (3.23)), and of SEEHAFER (1978, referred to as SEEP) (Equations (3.57a) - (3.57c)) have been applied to the same (line-of-sight) magnetogram (SEEHAFER, 1982). The used magnetogram (Fig. 1) was obtained at the Einstein tower telescope in Potsdam on 4 July, 1973, with a resolution of 7".5 : 6".0 and a scan area of 139" : 143" in the EW : NS directions, respectively. The value of the longitudinal field averaged over the magnetogram area is -88 G. The considered region is characterized by a large sunspot of p (-) polarity (towards S from the centre in Fig. 1). In the north of the spot a feature of f (+) polarity, elongated in EW direction and embedded in an area of opposite (-) polarity, moves away from the spot (ROY and MICHALITSANOS, 1974). In connection with this moving magnetic feature, some results of extrapolation using SEEP have already been published (SEEHAFER and STAUDE, 1980): At the northern boundary of the moving feature, where chromospheric activity (brightenings and ejections) was observed, an X-type neutral sheet (line) is situated.

For all three procedures, field lines have been calculated, starting from a mesh of photospheric foot points every 10" : 10", in the case of the two force-free procedures for several values of the parameter α. Figures 2 through 18 show the calculated lines of force in overview, perspective, and side (limb) view, in the case of the force-free procedures for three values of the parameter α, namely $\alpha = 0$ and $\pm 0.5\,\alpha_{max}$, where

$$\alpha^2_{max} = \pi^2 (L_x^{-2} + L_y^{-2}), \qquad (4.1)$$

L_x and L_y being the extents of the magnetogram in both directions. The main field structure, which is dominated by the large spot, is similar for all three procedures. On the other hand, in details there are differences, for example in the direction of the field lines in the overview (which is generally compared with Hα, EUV, and X-ray structures).

The domain of analysis has been the rectangular straight cylinder above the magnetogram area. For SEEP significantly more field lines leave this volume through the sides than for NRP and SCHP (look at the northern boundary in Fig. 9 - 11), for SCHP the number of such field lines being yet less than for NRP. Moreover, field lines calculated according to SCHP and NRP reach greater heights than those calculated using SEEP.

There is no simple correlation between the heights reached by the field lines and the field strength decrease with height, i. e., a higher reaching of the field lines is not necessarily connected with a slower decrease of the field strength. The height dependence of the maximum field strength calculated using the three procedures is displayed in Fig. 20. For NRP the field strength is significantly less than for SEEP and SCHP, for SCHP somewhat less than for SEEP.

The scale height of the magnetic field, defined by

$$z_m = \langle B_m \, (\partial B_m/\partial z)^{-1} \rangle, \qquad (4.2)$$

is a quantity of interest for many investigations, e. g. for studies of radio emission. In (4.2) B_m is the maximum field strength for a fixed height level z = const., and the triangular brackets denote an averaging over z. For $\alpha = 0$ we have z_m (NRP) : z_m (SCHP) : z_m (SEEP) = 1.0 : 1.5 : 1.8, while for $\alpha = 0.5\alpha_{max}$ z_m (NRP): z_m (SEEP) = 1 : 2, moreover, z_m ($\alpha = 0$) : z_m ($\alpha = 0.5\,\alpha_{max}$) = 1.0 : 1.1 for both NRP and SEEP. The reason for this behaviour will be discussed in the following section.

In Table I the magnetic energy contents of the region calculated according to the three procedures are compared. The differences are drastic, amounting to a factor of 10 between NRP and SCHP.

Table I: Magnetic energy (E) in 10^{32} erg

α	0	0.5	0.9
E (SEEP)	6.1	6.5	9.3
E (NRP)	2.2	2.3	2.5
E (SCHP)	19.3	-	-

5. Discussion

In Section 3.2.1.2. it has been shown that a magnetic field being force-free with α = constant ($\neq 0$) in the whole volume outside the Sun cannot have a finite energy content and cannot be determined uniquely from only one magnetic field component given at the photosphere. Therefore the extension of a global-scale constant-α force-free magnetic field to infinity neither has a physical meaning nor provides a mathematically unique boundary value problem. The use of global-scale constant-α force-free magnetic fields must be confined to the consideration of finite volumes. A generalization of the frequently used potential-field source-surface models, either with spherical (ALTSCHULER and NEWKIRK, 1969) or with non-spherical (SCHULZ et al., 1978) source-surface, to (non-

potential) force-free fields seems reasonable. Then, however, the parameter α cannot be a constant in the whole volume between the photosphere and the source-surface, since α must be zero at the source-surface (Section 3.2.1.2.). Since, furthermore, α is a constant along each field line, all open field lines must originate from current-free regions. Thus, in general, currents will be restricted to limited volumes with limited photospheric base, no field line leaving these volumes.

The start from global-scale magnetograms in extrapolating photospheric magnetic fields has the advantage (compared with the start from magnetograms covering limited regions) that no reference (in terms of special boundary conditions) to fields surrounding the magnetogram area is needed. Its disadvantage is the necessity to assume that the fields are steady for a period of about one month, which is needed to get a complete magnetic map of the photosphere. Thus the extrapolation starting from magnetograms covering limited regions is of interest. Moreover, this is the case so far as special assumptions, such as the constancy of α, are more questionable on a global scale.

If one computes the constant-α force-free magnetic field in the semi-infinite column above a limited photospheric region, it is inadequate to eliminate the need for boundary conditions on the vertical parts of the boundary byextending the volume into a half space, except for $\alpha = 0$. CHIU and HILTON (1977) have shown that the boundary value problem in a half space, using only the normal field component on the boundary as boundary values, is non-unique. It can be supposed that the result that a constant-α force-free magnetic field cannot have a finite energy content is also valid for the half space (the exact proof is mathematically non-trivial).

In the case of the extrapolation starting from magnetograms covering limited regions the boundary conditions must be treated carefully. The GREEN's function method given in Section 3.2.2.2. renders it possible to determine the constant-α force-free magnetic field (including the case $\alpha = 0$) above a limited photospheric region from boundary conditions on the surface enclosing the actually considered volume. Different boundary conditions, especially those considered as realistic for physical reasons, can be imposed, the presently used extrapolation methods being included as special cases in the derived general scheme. The practical use of the scheme has been illustrated in deriving our extrapolation procedure (SEEP) which uses boundary conditions somewhat different from those of the procedure of NAKAGAWA and RAADU (NRP) and, therefore, does not require the net magnetic flux through the magnetogram area to be zero.

From a comparison of NRP and the SCHMIDT procedure (SCHP) LEVINE (1975) concluded that prohibiting field lines from leaving the volume through the sides causes them to become longer and higher. He found that field lines calculated using SCHP tend to extend higher and to start and to end on the magnetogram area. In fact, for SCHP field lines starting from the magnetogram must return to it. This is because for this procedure the actual volume for which the used solution holds is the half space above the plane of magnetograph observation, the field component normal to the boundary plane vanishing everywhere outside the magnetogram area itself. In the example of an application of SEEP, NRP, and SCHP to the same magnetogram presented in Section 4., also for SCHP field line tracing has been terminated at the sides of the rectangular column above the magnetogram area. For this reason in Figures 4, 11, and 18 some field lines seem to leave the region.

Also in the example presented in Section 4., for NRP, which allows for field lines starting from the magnetogram area without returning to it, some more field lines leave the volume than for SCHP, however yet much less than for SEEP. This is due to the fact that both SCHP and NRP assume the net magnetic flux through the magnetogram area, which must be connected to flux outside this area, to be zero, which SEEP does not. SCHP and NRP neglect the net magnetic flux through the magnetogram area, i. e., they do not start from the real magnetogram but from one which is got from the real one by substracting the mean (vertical) field value, -88 G in the considered case. This value is relatively large and one may ask if SCHP and NRP are applicable here, but for a methodical study such a magnetogram is well suited.

Of course, field lines leaving the studied volume must be considered with caution. However, field lines staying inside the volume also do not necessarily have a conclusive meaning. Whether or not a field line leaves the volume depends on the applied boundary conditions, and the staying inside of a field line may have been caused by boundary conditions which differ from those on the Sun. Thus prohibiting field lines from leaving the studied volume does not increase the reliability of an extrapolation procedure.

SEEP does not assume flux balance over the magnetogram area. The magnetic field is calculated from the magnetogram and the condition that the vertical field component vanishes on the sides of the considered rectangular cylinder, i. e., the condition that the field is horizontally directed there. By these boundary conditions the information contained in the magnetogram on those field lines leaving the volume becomes usable to some extent. It is not so that this is reached by replacing the flux balance condition of NRP by the condition on the vertical field component at the vertical boundary of SEEP. NRP, in addition to the flux balance condition, implies a condition at the vertical boundary as restrictive as that of SEEP (SEEHAFER, 1975, 1978; cf.; Section 3.2.2.1.). For both procedures these conditions at the vertical boundary may be expressed by requiring the FOURIER expansions representing the two solutions to be twice differentiable term by term. The difference between SEEP and NRP results from the different choice of the set of eigenfunctions in which the solutions are expanded.

The observed differences between the three procedures in the direction and location of field lines are in part due to the fact that SCHP and NRP start from a fictive magnetogram. Compared with the real magnetogram the zero lines are displaced and with them field lines bridging over them.

With increasing horizontal scale length of the magnetic field the field strength decrease with height will become slower. The horizontal scale length of the solution used in SEEP is larger than that of the solution used in NRP (Section 3.2.2.2.), that of the solution used in SCHP being yet larger (infinite). Thus in Figure 20 the curve for SEEP should lie between those for NRP and SCHP. That this is not the case is due to the fact that NRP and SCHP start from a magnetogram in which the absolute value of the maximum vertical field strength is reduced by 88 G. This leads to reduced total vector field strengths also above the magnetogram plane. For magnetograms with small mean (vertical) field values the curve for SEEP should become located below that for SCHP.

As to the calculations of the magnetic energy content of the region (Table I) it must be mentioned that for SCHP the volume of calculation is not, as for NRP and SCHP, the rectangular cylinder above the magnetogram, but the whole half space in which the used solution is valid (Equation (4) of SCHMIDT (1964)). This is the only reason for the magnetic energy corresponding to SCHP being so large compared with the energies corresponding to SEEP and NRP, since from the field strength decrease above the magnetogram (Figure 20) for SCHP an energy less than that for SEEP would follow.

One may ask if also for SCHP only the magnetic energy in the column above the magnetogram area should be considered. However, for a separation of different parts of the magnetic energy to have a physical meaning, it must be based on information about the electric currents causing the magnetic field, which is not available.

In this context it should be noted that the physical meaning of the energy content of a potential field above the photosphere is not very clear, since the generating electric currents flow below the photospheric level and a separation of magnetic energies above and below this level is not justified.

The excess energy (compared with the potential field) of a force-free magnetic field above the photosphere, on the other hand, has a clear physical meaning, since it is due to atmospheric electric currents. For both SEEP and NRP the lateral boundary conditions are such that for the magnetic field to vanish at infinity the absolute value of the parameter α must be less than a maximum value, for SEEP this maximum value being somewhat smaller than for NRP. In Table I α_{max} denotes the maximum value for SEEP. As $|\alpha|$

approaches the maximum value the magnetic energy becomes infinite. This explains why with $|\alpha|$ increasing the ratio of the magnetic energies corresponding to SEEP and NRP increases. On the other hand it shows that the boundary conditions may have a greater influence on the excess energy stored than the value of α.

Throughout the present review the force-free parameter α has been assumed to be spatially constant. For non-constant α the problem remains tractable, because it remains linear, if $\alpha(\underset{\sim}{r})$ is prescribed (PICARD, 1976; KRESS, 1977). This, however, requires information on α inside the considered volume or, since the field lines lie in the surfaces α = const., on the field line geometry. The non-linear boundary value problem for a general force-free magnetic field, on the other hand, is presently not tractable; even what are the proper boundary conditions is not known. In fusion research iterative procedures based on a variational principle are used to calculate (stable) magneto-hydrostatic equilibria (CHODURA et al., 1979). Maybe these procedures can, at least in part, become usable for the present problem. Recently SAKURAI (1981) has presented an iteration procedure for the calculation of force-free magnetic fields with non-constant α. This procedure, which is based on a theorem given by BINEAU (1972), requires the specification of the normal magnetic field component on the whole boundary and of α on a part of the boundary and converges for $|\alpha(\underset{\sim}{r})|$ sufficiently small. It seems that this shows the way in which further progress in the force-free solar magnetic field problem may be reached.

References

ADAMS, J., and PNEUMAN, G. W.: 1976, Solar Phys. 46, 185.

ALTSCHULER, M. D., and NEWKIRK, G. Jr.: 1969, Solar Phys. 9, 131.

ALTSCHULER, M. D., LEVINE, R. H., STIX, M., and HARVEY, J.: 1977, Solar Phys. 51, 345.

ANGER, G. (ed.): 1979, Conference on Mathematical and Numerical Methods for Inverse and Improperly Posed Problems in Differential Equations, Mathematical Research 1, Akademie-Verlag, Berlin

BACHMANN, G., JÄGER, F. W., KÜNZEL, H., PFLUG, K., and STAUDE, J.: 1975, HHI-STP-Report No. 4, Zentralinstitut für solar-terrestrische Physik, Berlin

BARBOSA, D. D.: 1978a, Astron. Astrophys. 62, 267.

BARBOSA, D. D.: 1978b, Solar Phys. 56, 55.

BECKERS, J. M.: 1971, in R. HOWARD (ed.), 'Solar Magnetic Fields', IAU Symp. 43, 3.

BINEAU, M.: 1972, Comm. Pure Appl. Math. 25, 77.

BÖHME, A., FÖRSTENBERG, F., HILDEBRANDT, J., HOYNG, P., KRÜGER, A., SAAL, O., and STEVENS, G. A.: 1976, HHI-STP-Report No. 6, Zentralinstitut für solar-terrestrische Physik, Berlin

BOSTRÖM, R.: 1973, Astrophys. Space Sci. 22, 353.

BROMBOSZCZ, G., JAKIMIEC, J., SIARKOWSKI, M., SYLVESTER, B. and J., OBRIDKO, V., FÖRSTENBERG, F., HILDEBRANDT, J., KRÜGER, A., and STAUDE, J.: 1981a, Physica solari-terr. 16, 155 = Proc. 10th Consultation on Solar Physics, Potsdam 1980; 1981b, Proc. SMY Workshop, Crimea, Vol. 1, 224; 1982, IZMIRAN, Moscow, Preprint No. 11a

CHANDRASEKHAR, S.: 1961, Hydrodynamic and Hydromagnetic Stability, Clarendon Press, Oxford, p. 622.

CHAPMAN, S., and BARTELS, J.: 1940, "Geomagnetism", Oxford University Press, London.

CHIU, Y. T., and HILTON, H. H.: 1977, Astrophys. J. 212, 873.

CHODURA, R., SCHLÜTER, A., KAUFMANN, M., and LÖTZ, W.: 1979, in "Plasma Physics and Controlled Nuclear Fusion Research 1978", Vol 2, International Atomic Energy Agency, Vienna, p. 335.

GAIL, H.-P.: 1969, Abhandl. Hamburger Sternwarte VIII Nr. 6, 185.

GEBBIE, K. B., and STEINITZ, R.: 1973, Solar Phys. 29, 3.

GELFREIKH, G. B., and LUBYSHEV, B. I.: 1979, Astron. Zh. 56, 562.

GOPASYUK, S. I.: 1979, Izv. Krymsk. Astrofiz. Obs. 60, 108.

HAGYARD, M., LOW, B. C., and TANDBERG-HANSSEN, E.: 1981, Solar Phys. 73, 257.
HARVEY, J.: 1977, in E. A. JÜLLER (ed.), Highlights of Astronomy 4/II, 223.
KNOPS, R. J. (ed.): 1973, Symposium on Non-Well-Posed Problems and Logarithmic Convexity, Lecture Notes in Mathematics 316, Springer, Berlin
KRESS, R.: 1977, J. Appl. Math. Phys. (ZAMP) 28, 715.
KRÜGER, A.: 1979, 'Introduction to Solar Radio Astronomy and Radio Physics', Dr Reidel, Dordrecht-Holland.
LAMB, F. K.: 1972, 'Line Formation in the Presence of Magnetic Fields', NCAR, Boulder, Colorado, p. 1.
LAVRENTIEV, M. M.: 1967, 'Some Improperly Posed Problems in Mathematical Physics', Springer Tracts in Natural Philosophy 11, Springer, Berlin-Heidelberg-New York.
LEROY, J. L.: 1977, Astron. Astrophys. 60, 79.
LEVINE, R. H.: 1975, Solar Phys. 44, 365.
MÜLLER, C.: 1969, 'Foundations of the Mathematical Theory of Electromagnetic Waves', Springer, New York.
NAKAGAWA, Y.: 1973, Astron. Astrophys. 27, 95.
NAKAGAWA, Y., and RAADU, M. A.: 1972, Solar Phys. 25, 127.
PICARD, R.: 1976, J. Appl. Math. Phys. (ZAMP) 27, 169.
PNEUMAN, G. W., and KOPP, R. A.: 1971, Solar Phys. 18, 258.
RÄDLER, K.-H.: 1974, Astron. Nachr. 295, 73.
RELLICH, F.: 1943, Jber. Deutsch. Math. Verein 53, 57.
RIESEBIETER, W., and NEUBAUER, F. M.: 1979, Solar Phys. 63, 127.
ROY, J.-R., and MICHALITSANOS, A. G.: 1974, Solar Phys. 35, 47.
SAHAL-BRECHOT, S., BOMMIER, V., and LEROY, J. L.: 1977, Astron. Astrophys. 59, 223.
SAKURAI, T.: 1981, Solar Phys. 69, 343.
SAKURAI, T.: 1982, Solar Phys. 76, 301.
SCHATTEN, K. H., WILCOX, J. M., and NESS, N. R.: 1969, Solar Phys. 6, 442.
SCHMIDT, H. U.: 1964, in AAS-NASA Syposium on the Physics of Solar Flares, NASA SP-50, 107.
SCHOOLMAN, S. A.: 1972, Solar Phys. 22, 344.
SCHULZ, M., FRAZIER, E. N., and BOUCHER, D. J., Jr.: 1978, Solar Phys. 60, 83.
SEEHAFER, N.: 1975, Astron. Nachr. 296, 177.
SEEHAFER, N.: 1978, Solar Phys. 58, 215.
SEEHAFER, N.: 1979, "Theoretische Extrapolation photosphärischer Magnetfelder als Beitrag zur Ermittlung der magnetischen Struktur solarer aktiver Regionen", Ph. D. Thesis, Akademie der Wissenschaften der DDR, Berlin.
SEEHAFER, N.: 1980, Phys. Solariterr. 13, 95.
SEEHAFER, N.: 1982, Solar Phys. 81, 69.
SEEHAFER, N., and STAUDE, J.: 1977, Publ. Debrecen Heliphys. Observ. 3, 137.
SEEHAFER, N., and STAUDE, J.: 1979, Astron. Nachr. 300, 151.
SEEHAFER, N., and STAUDE, J.: 1980, Solar Phys. 67, 121.
SENEL, M.: 1967, Ann. Astrophys. 30, 513.
STAUDE, J.: 1974, Z. Meteorologie 24, 214.
STAUDE, J.: 1980, Physica solariterr. 14, 58.
STEINITZ, R., GEBBIE, K. B., and BAR, V.: 1977, Astrophys. J. 213, 269.
STENFLO, J. O.: 1971, in R. HOWARD (ed.), 'Solar Magnetic Fields', IAU Symp. 43, 101.
STENFLO, J. O.: 1978, Rep. Prog. Phys. 41, 865.
SWEBROCK, P. A., and WOODBURY, E. T.: 1967, in "Plasma Astrophysics", 39th Enrico Fermi School, Academic Press, New York, p. 155.
TANDBERG-HANSSEN, E., ATHAY, R. G., BECKERS, J. M., BRANDT, J. C., BRUNER, E. C., CHAPMAN, R. D., CHENG, C. C., GURMAN, J. B., HENZE, W., HYDER, C. L., MICHALITSIANOS, A. G., SHINE, R. A., SCHOOLMAN, S. A., and WOODGATE, B. E.: 1981, Astrophys. J. 244, L. 127.
WEBER, D., TANDBERG-HANSSEN, E., and HAGYARD, M. J.: 1977, Solar Phys. 53, 97.

WELLCK, R. E., and NAKAGAWA, Y.: 1973, NCAR Technical Note, Boulder, STR-87.
WITTMANN, A.: 1974, Solar Phys. 35, 11.
YEH, T., and PNEUMAN, G. W.: 1977, Solar Phys. 54, 419.
ZELENKA, A.: 1975, Solar Phys. 40, 39.

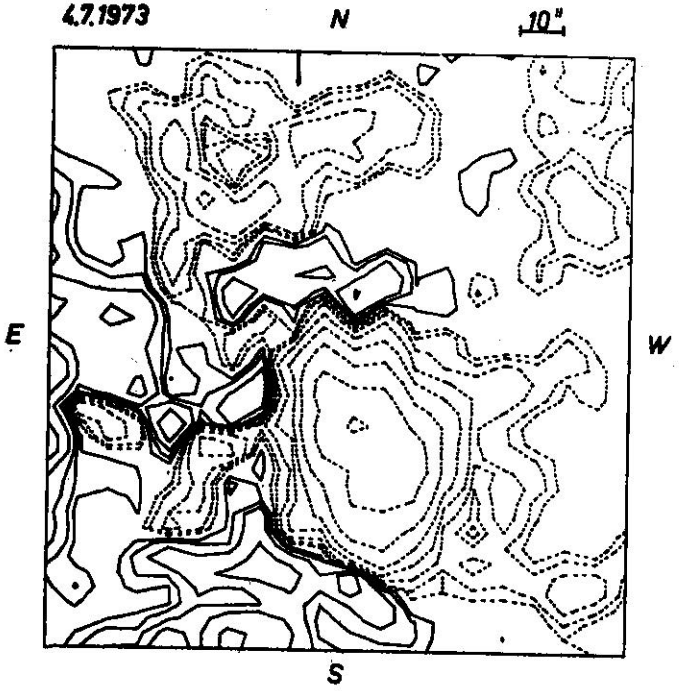

Fig. 1: Photoelectric magnetogram (B_ℓ) obtained at the Solar Observatory Einsteinturm in Potsdam on 4 July, 1973, 0830 UT. Contour levels are 20, 40, 80, 160, 320, 640, 1280, and 2560 G. Solid and dashed lines refer to positive and negative polarities, respectively.

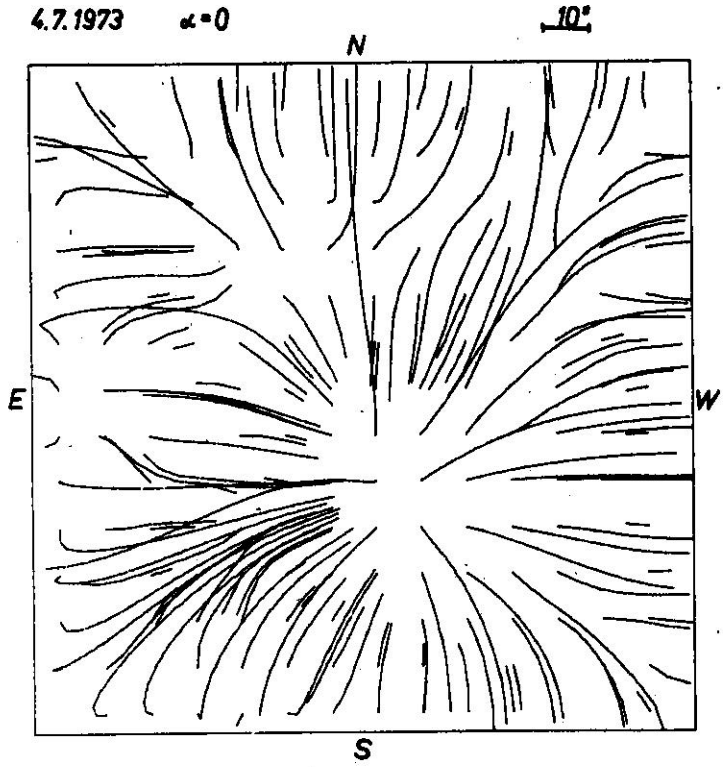

Fig. 2: Overview of the field lines of a potential field, calculated using the SEEHAFER procedure.

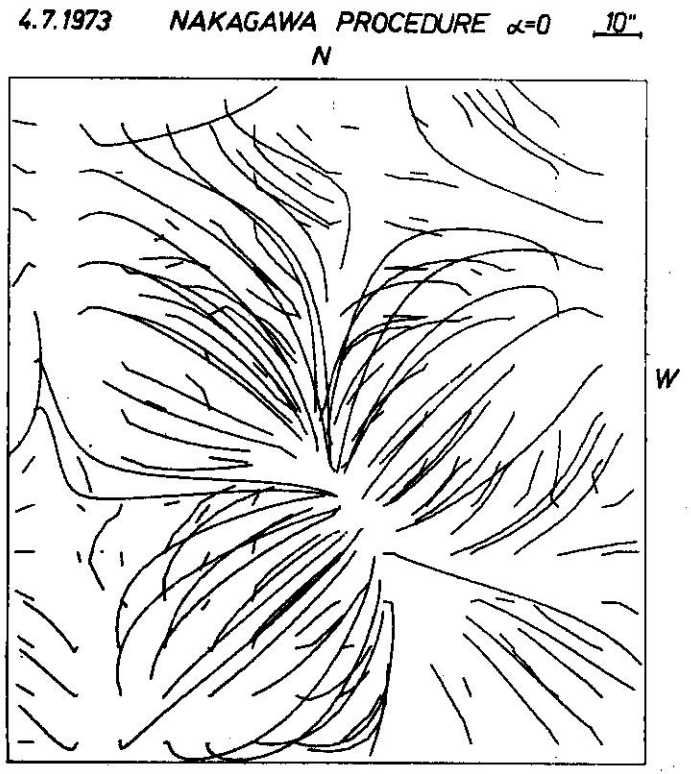

Fig. 3: Overview of the field lines of a potential field, calculated using the NAKAGAWA and RAADU procedure.

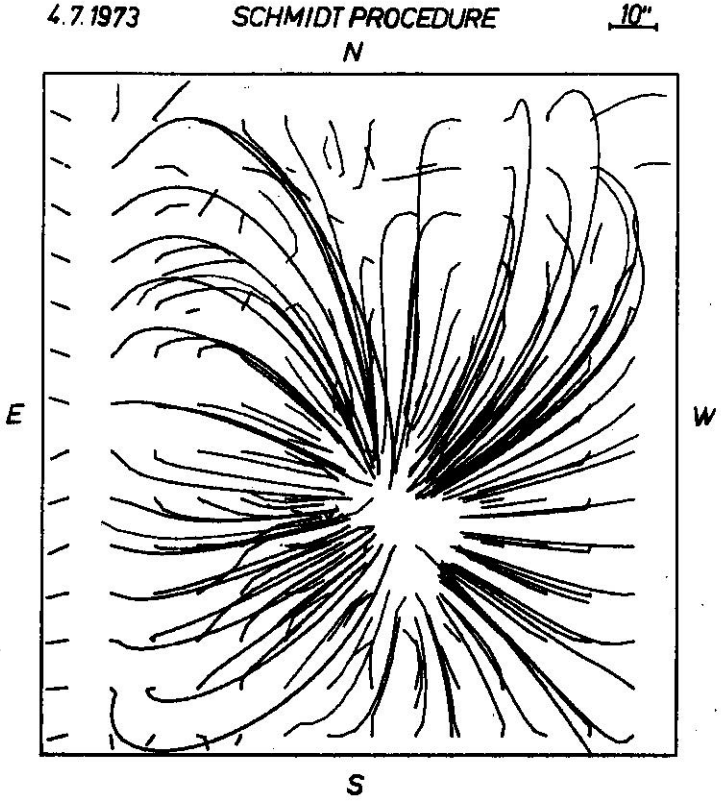

Fig. 4: Overview of the field lines calculated using the SCHMIDT procedure.

Fig. 3: Overview of the field lines of a potential field, calculated using the NAKAGAWA and RAADU procedure.

Fig. 4: Overview of the field lines calculated using the SCHMIDT procedure.

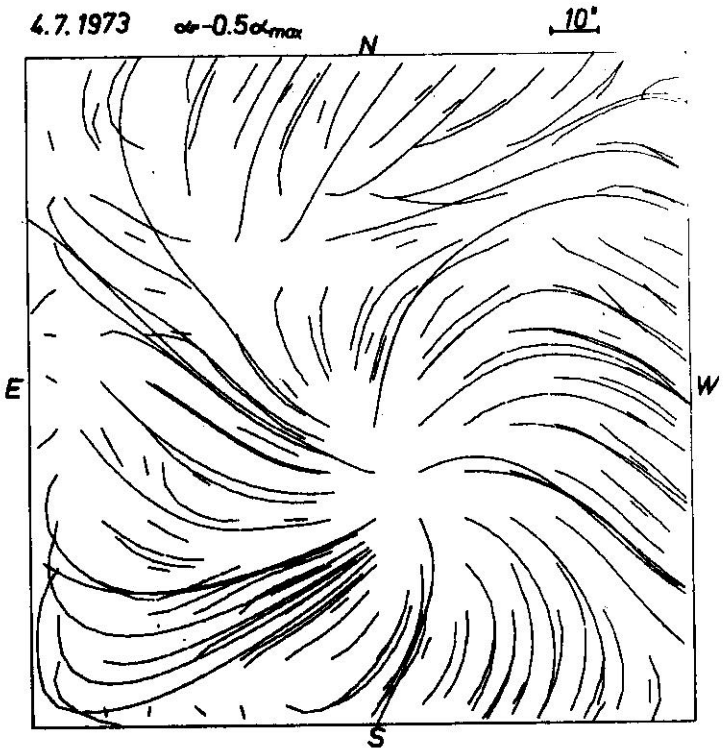

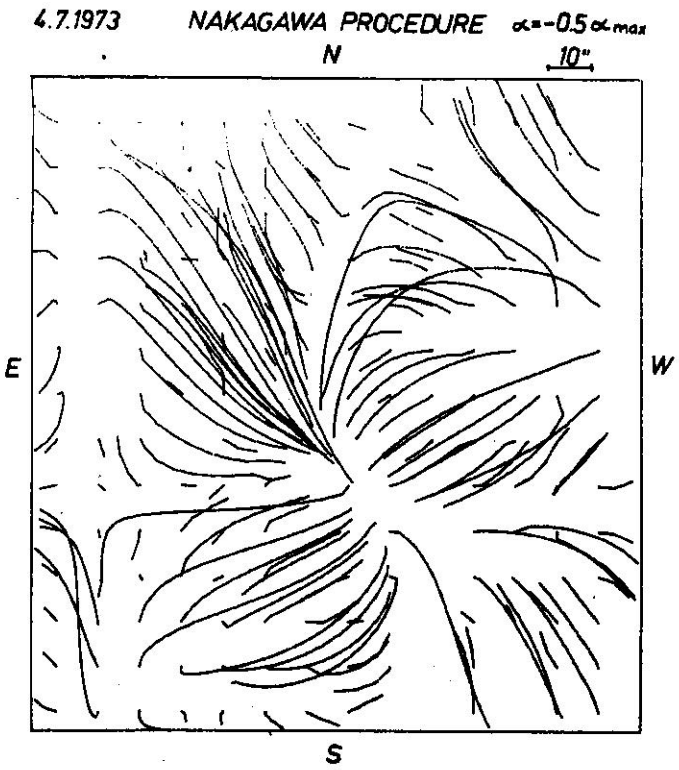

Fig. 5: Overview of the field lines of a force-free field with $\alpha = -0.5\alpha_{max}$, calculated using the SEEHAFER procedure.

Fig. 6: Overview of the field lines of a force-free field with $\alpha = -0.5\alpha_{max}$, calculated using the NAKAGAWA and RAADU procedure.

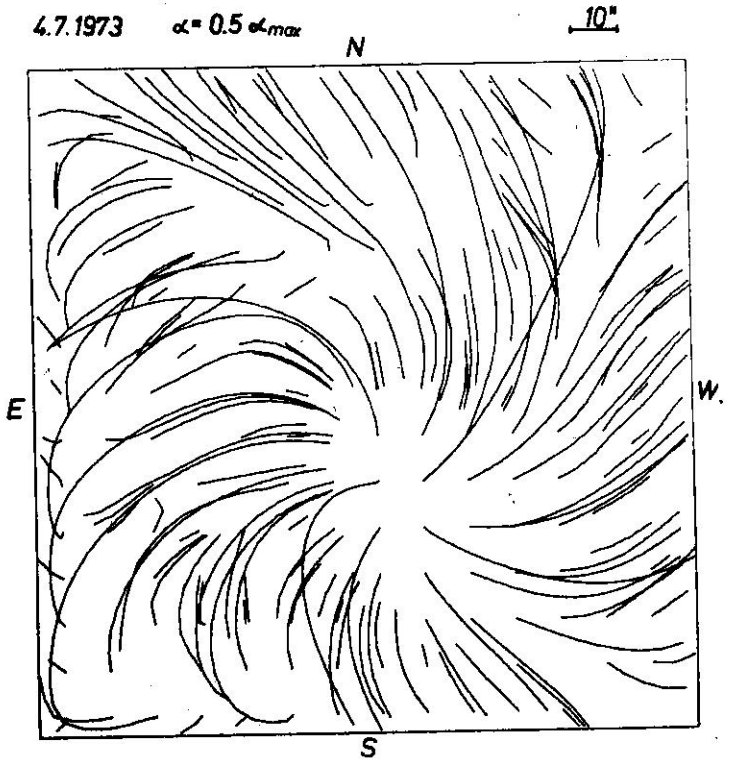

Fig. 7: Overview of the field lines of a force-free field with $\alpha = +0.5\,\alpha_{max}$, calculated using the SEEHAFER procedure.

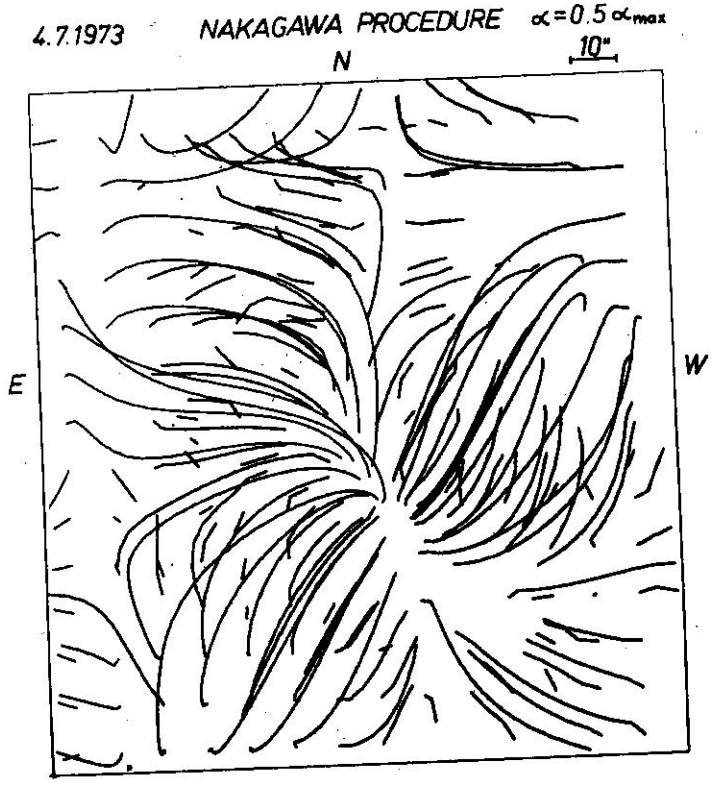

Fig. 8: Overview of the field lines of a force-free field with $\alpha = +0.5\,\alpha_{max}$, calculated using the NAKAGAWA and RAADU procedure.

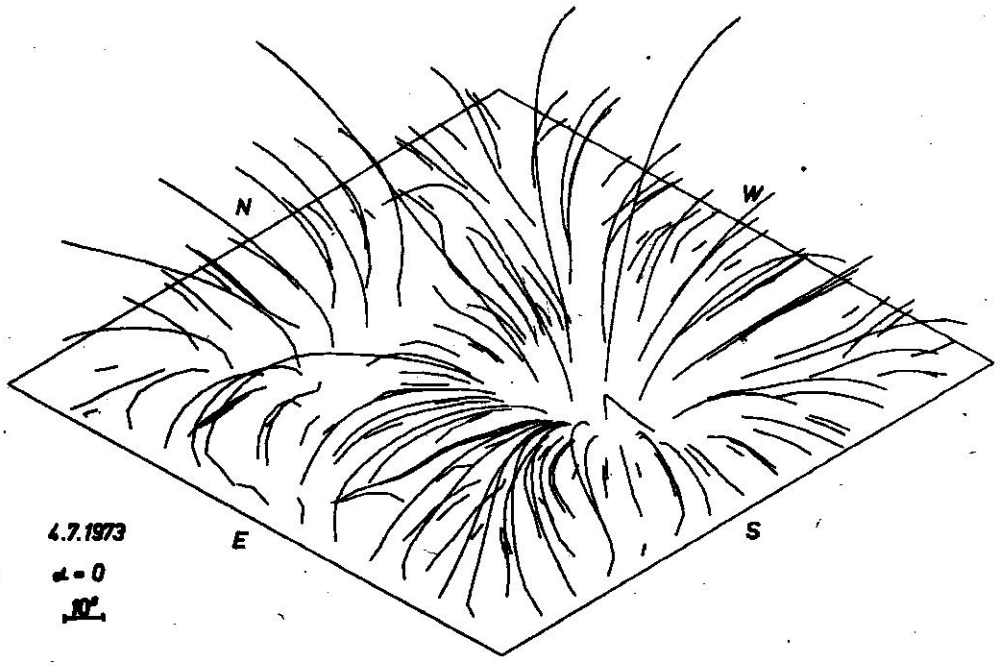

Fig. 9: Perspective view of the field lines of Fig. 2,

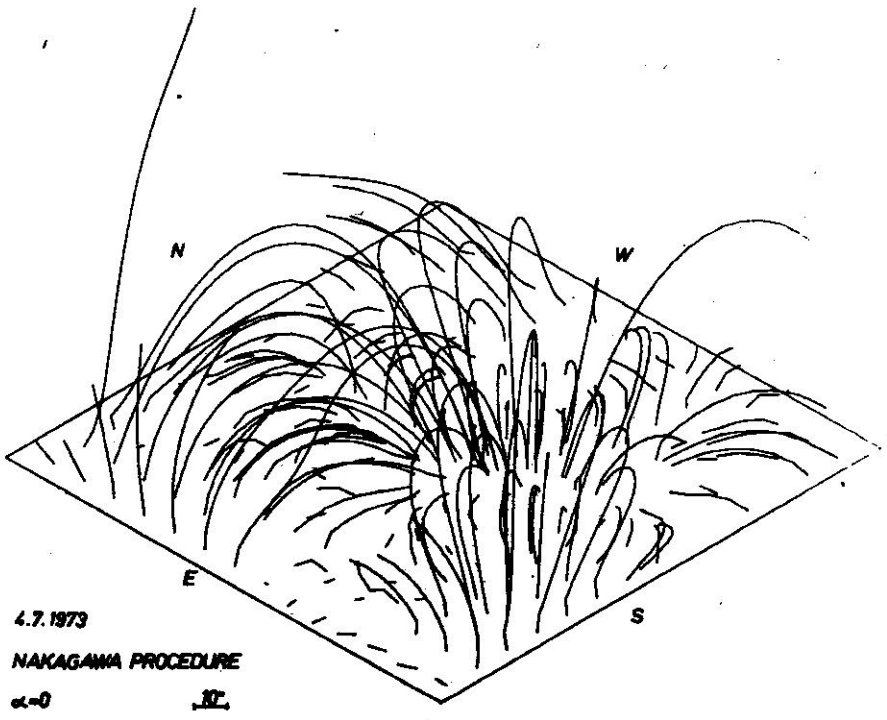

Fig. 10: Perspective view of the field lines of Fig. 3.

Fig. 8: Overview of the field lines of a force-free field with $\alpha = +0.5\,\alpha_{max}$, calculated using the NAKAGAWA and RAADU procedure.

Fig. 7: Overview of the field lines of a force-free field with $\alpha = +0.5\,\alpha_{max}$, calculated using the SEEHAFER procedure.

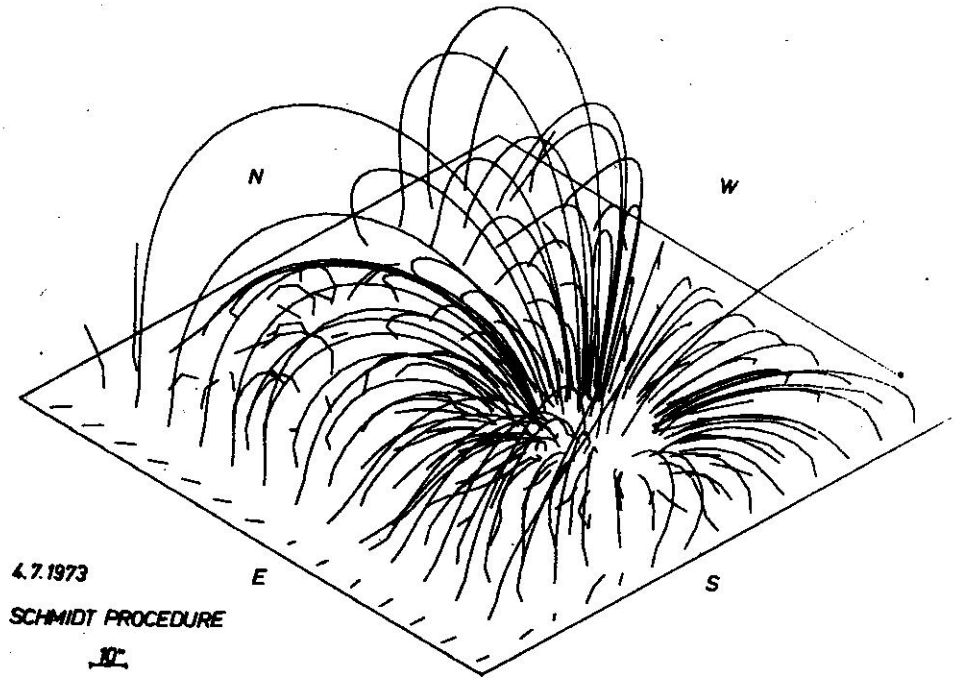

Fig. 11: Perspective view of the field lines of Fig. 4.

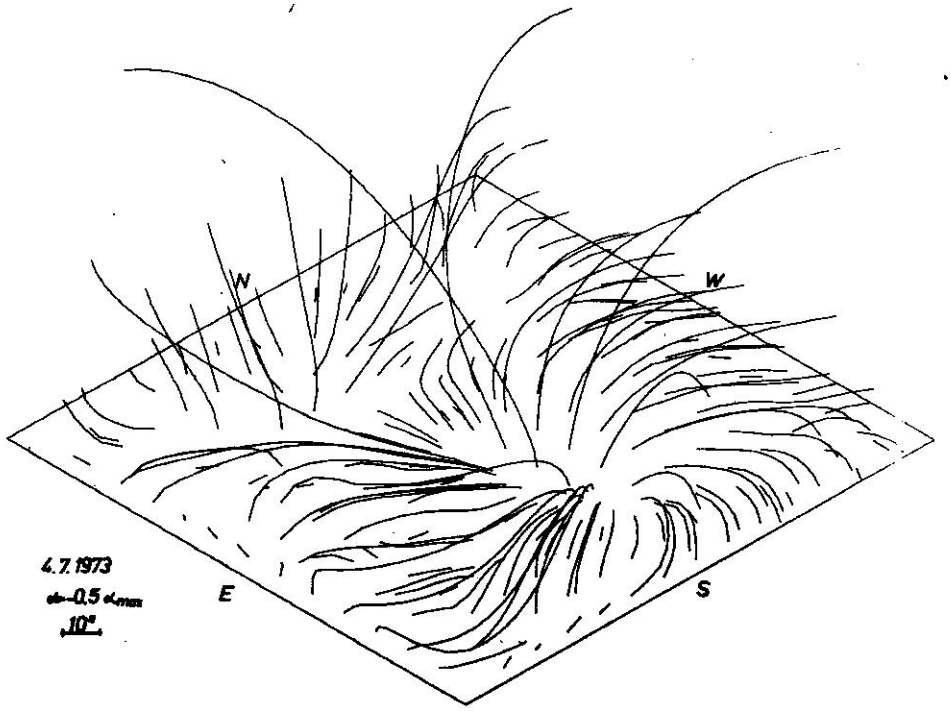

Fig. 12: Perspective view of the field lines of Fig. 5.

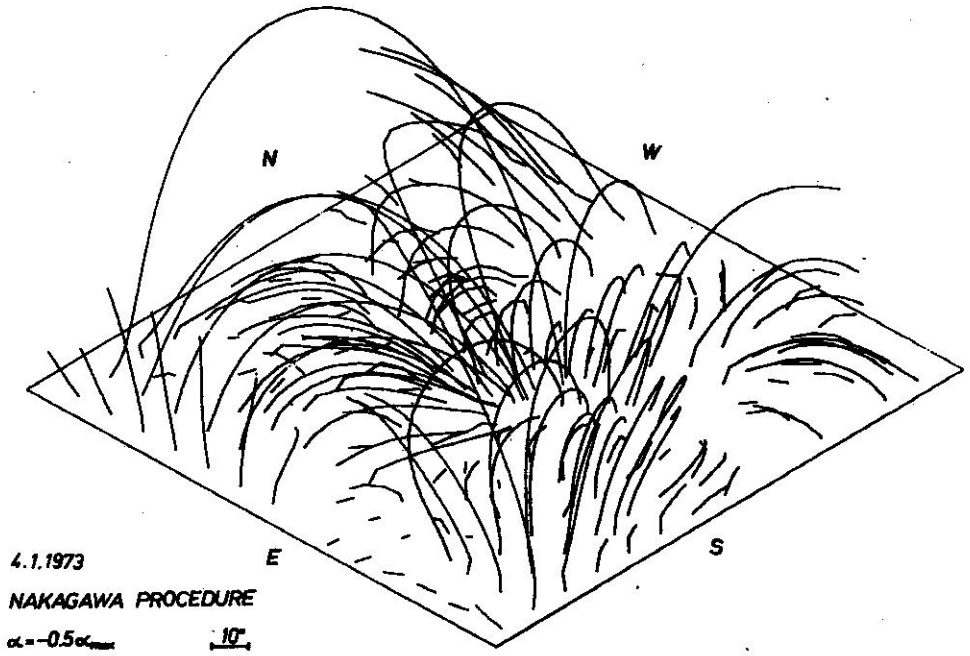

Fig. 13: Perspective view of the field lines of Fig. 6.

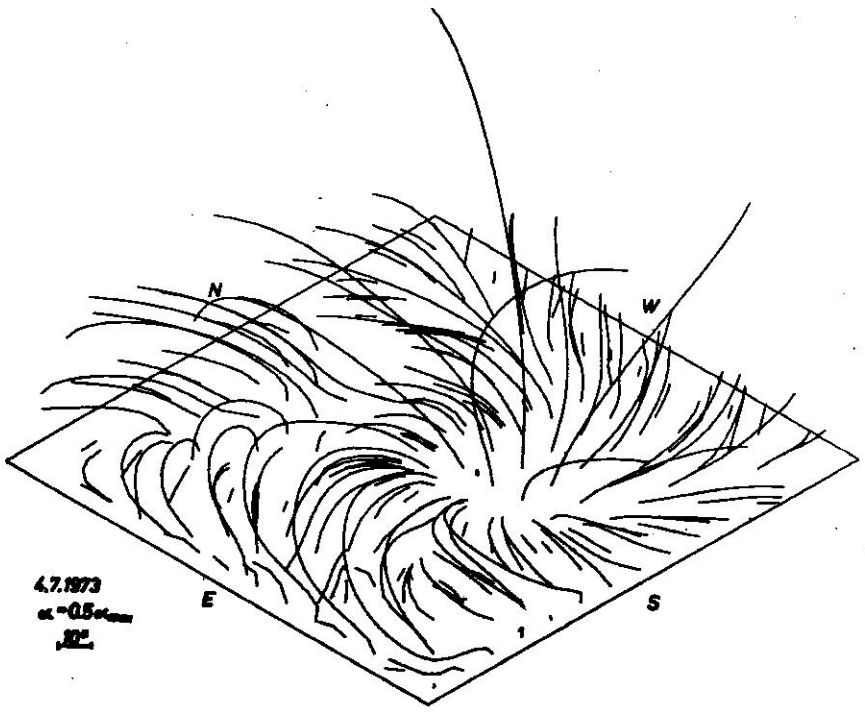

Fig. 14: Perspective view of the field lines of Fig. 7.

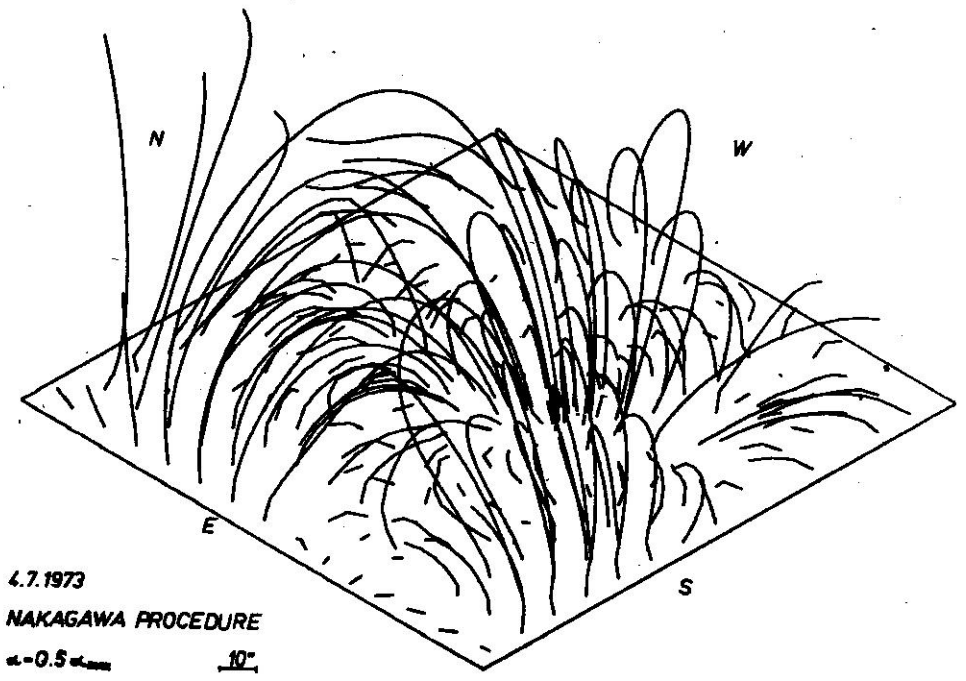

Fig. 15: Perspective view of the field lines of Fig. 8,

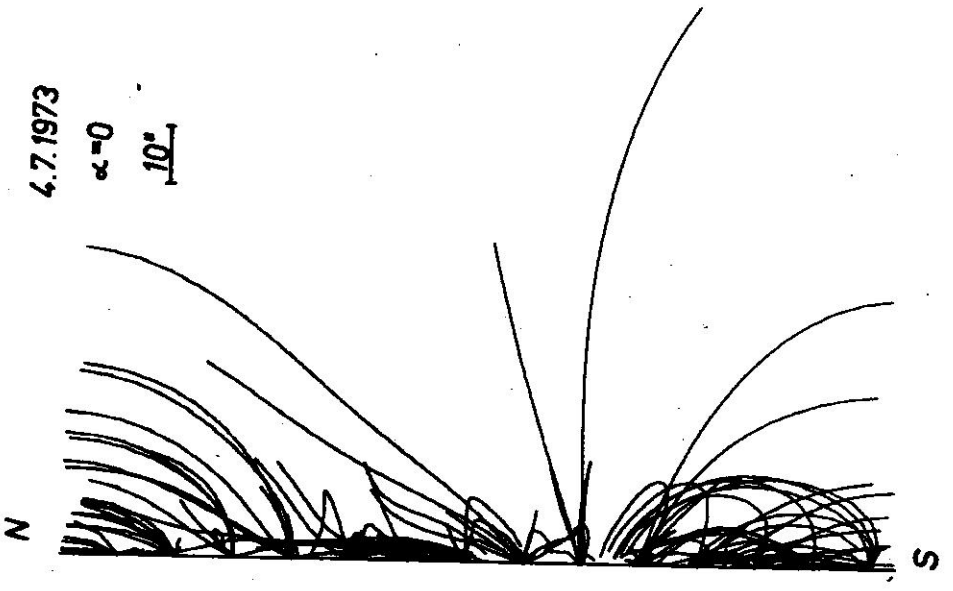

Fig. 16: Side view of the field lines of Fig. 2.

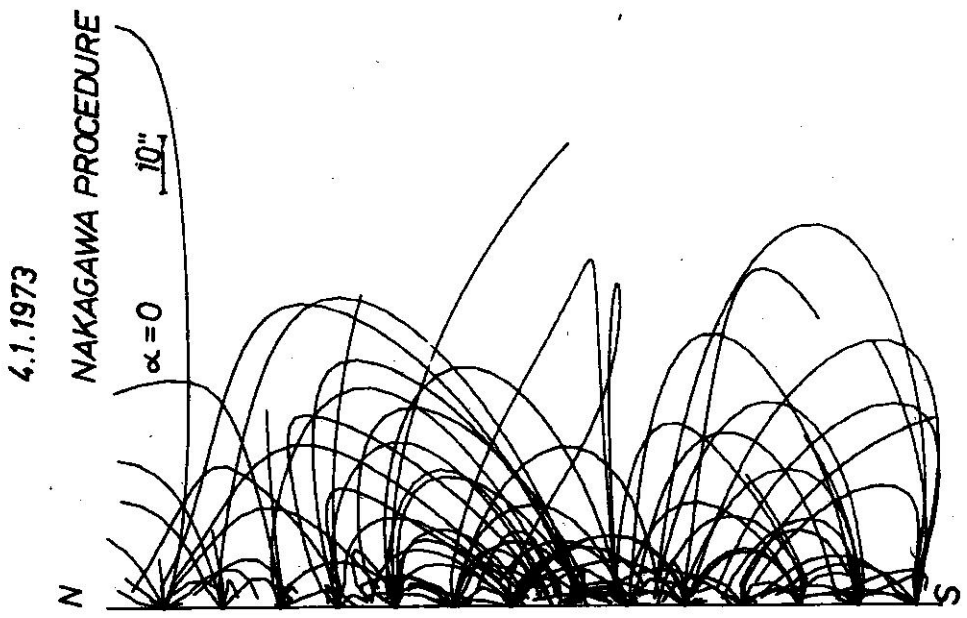

Fig. 17: Side view of the field lines of Fig. 3.

Fig. 18: Side view of the field lines of Fig. 4.

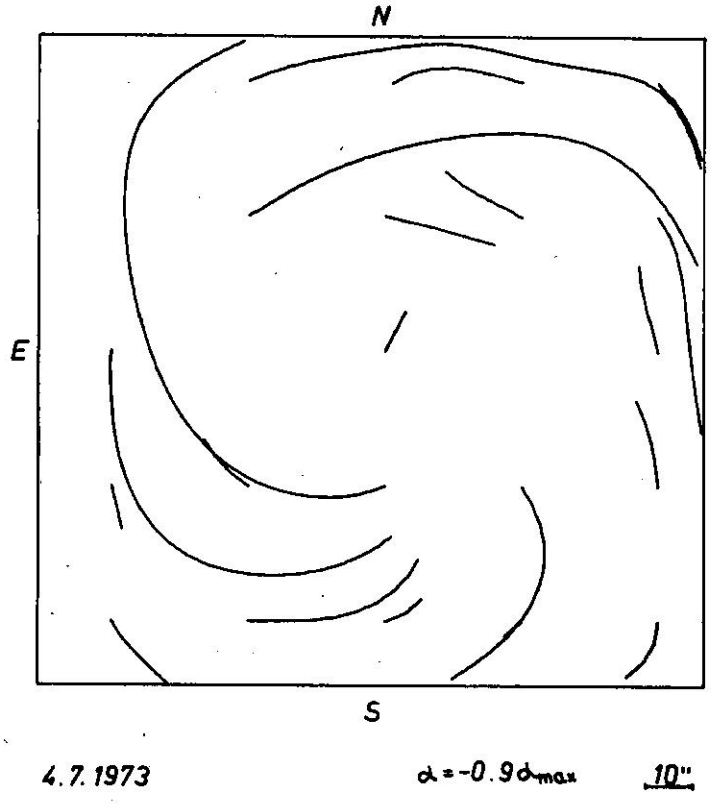

Fig. 19: Overview of the field lines of a force-free field with $\alpha = -0.9\,\alpha_{max}$, calculated using the SEEHAFER procedure.

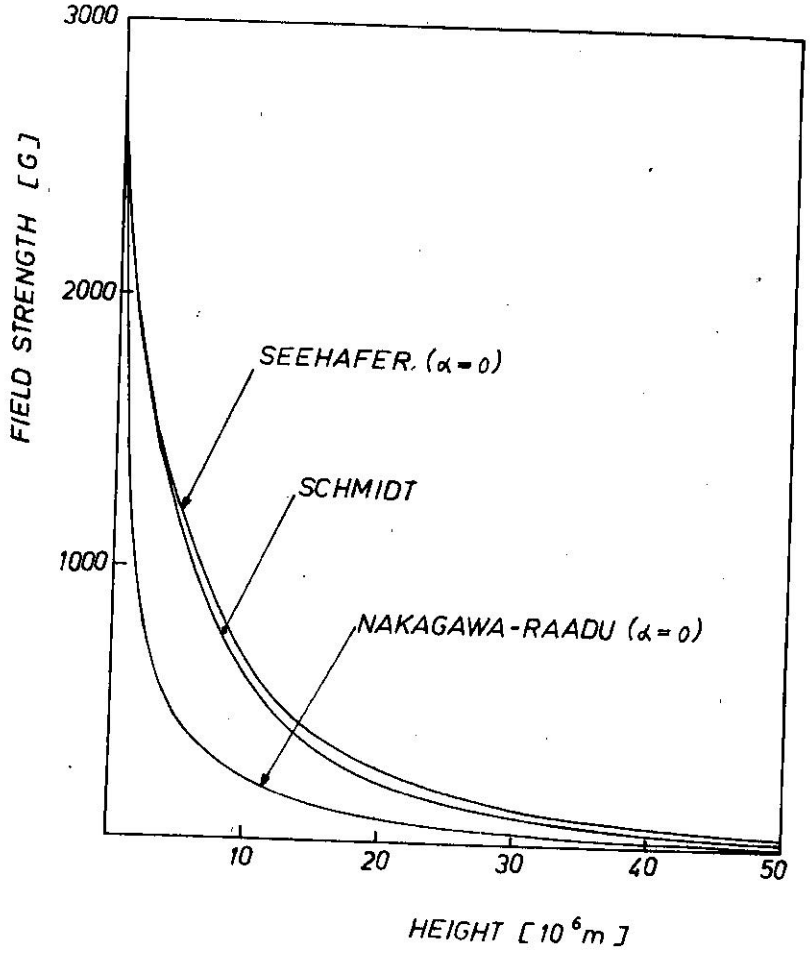

Fig. 20: Height dependence of the maximum field strength B_m of each one height level for a potential field calculated according to the SEEHAFER, NAKAGAWA-RAADU, and SCHMIDT procedures.